BEHAVIOR OF ONE-WAY RC SLABS FLEXURALLY STRENGTHENED WITH PRESTRESSED NSM CFRP LAMINATES - ASSESSMENT OF INFLUENCING PARAMETERS

M. R. Mostakhdemin Hosseini, S. J. E. Dias and J. A. O. Barros

ISISE, Institute of Science and Innovation for Bio-Sustainability (IB-S), Department of Civil Engineering, University of Minho, Guimarães, Portugal

ABSTRACT

The efficacy of the NSM technique using prestressed CFRP laminates for the flexural strengthening of RC slabs was assessed experimentally. The results obtained indicated that the application of NSM CFRP laminates with a certain level of prestress is a suitable strategy to increase the load-carrying capacity of slabs in terms of service limit state (SLS) conditions. The higher is the CFRP prestressed level the larger is the performance of the NSM technique in the improvement of the behavior of the slabs at SLS conditions, but the deflection at the maximum load of the slabs decreased with the increase of the prestress level. The prestressed NSM CFRP laminates were more effective in the slabs with the lower concrete strength class, mainly at SLS conditions. The increase of the percentage of the flexural reinforcement had a detrimental effect on the performance of prestressed NSM CFRP laminates. An analytical formulation was developed for predicting the cracking, yielding and maximum loads of RC slabs flexurally strengthened with prestressed NSM CFRP laminates and a very good predictive performance was obtained. An upper limit is proposed for the prestress level for ensuring a compromise of ductility and strengthening effectiveness of this type of structural elements.

KEYWORDS: Prestressed CFRP laminates, NSM technique, RC slabs flexurally strengthened, Experimental results, Analytical approach

1. INTRODUCTION

The application of CFRP (carbon fiber reinforced polymer) materials for the repair or for the strengthening of RC (reinforced concrete) members has augmented considerably during the last few decades due to the high durability (immunity to corrosion), excellent strength-to-weight and stiffness-to-weight ratios, electromagnetic neutrality, fast execution with low labor, easy to handle, and unlimited access in geometry, size and dimension of these advanced composite materials [1].

The two major techniques in terms of the flexural strengthening of RC structural elements with CFRP are EBR (Externally Bonded Reinforcement) and NSM (Near Surface Mounted). In the EBR technique, laminates or sheets are bonded to external tension surfaces of the elements [2-5], while in the NSM technique, circular, rectangular or square cross section CFRP bars are installed into pre-cut slits opened on the concrete cover of the elements to be strengthened [4-11].

Based on experimental research, the strengthening effectiveness of the NSM technique is higher than the EBR technique, mainly when slender rectangular cross section of CFRP laminates are used in the NSM technique [4, 5, 7]. This fact is justified by the better CFRP-concrete bond performance (higher surface of the CFRP bonded to concrete substrate regarding its cross section) that can be mobilized in the NSM technique with CFRP laminates, which provides a more efficient use of the CFRP (increase of the ratio of CFRP strain at failure to its maximum strain) [12]. Furthermore, as a consequence of the protection of the CFRP by the concrete cover, NSM technique reduce significantly the probability of mechanical damage, harm resulting from acts of vandalism, and aging effects. NSM does not require surface preparation work and, after cutting the thin slits where the CFRP laminates are installed (a single saw cut is normally enough for obtaining the slit), requires relatively small installation time.

Several experimental programs have been carried out to assess the performance of RC beams [4-10] and slabs [13-14] flexurally strengthened with passive NSM CFRP laminates. These studies demonstrated that the use of passive NSM CFRP laminates increases significantly the load carrying capacity of RC structural elements for the ultimate limit states (ULS) conditions (with a very effective mobilization of the high tensile properties of the CFRP). However, its overall performance for deflection levels corresponding to the serviceability limit state (SLS) conditions is only slightly improved. Applying prestress in the NSM CFRP laminates for flexural strengthening can increase significantly the load carrying capacity of the RC structural elements not only in SLS but also in ULS conditions [15-20]. The prestress can also contribute for closing existing cracks, to decrease the number and width of cracks that can be formed in SLS, to decrease the tensile stress in the existing flexural reinforcement, and increase the shear capacity of these elements. Thus, a cost-effective solution to increase, not only the structural performance, but also the durability of the strengthened RC structures seems to be the application of prestressed CFRP laminates.

In this study, the effectiveness of the NSM technique with prestressed CFRP laminates for the flexural strengthening of one-way RC slabs was assessed by executing an extensive experimental research. In this context, the influence of the CFRP prestress level, the concrete strength and the percentage of existing flexural reinforcement was appraised. The experimental program carried out is described in detail (slab specimens, series of tests, materials properties, test setup and monitoring system), the results of the tests are displayed and discussed, and the derived relevant conclusions are pointed out. The performance of a proposed analytical formulation to predict the cracking, yielding and maximum loads of the tested RC slabs flexurally strengthened with prestressed NSM CFRP laminates is assessed. Furthermore, a methodology is proposed to obtain an upper limit of the prestress level applicable to the CFRP laminates that assures a suitable compromise between ductility and load carrying capacity. A parametric study was also executed to highlight the influence of the percentage of existing tensile flexural reinforcement and the concrete strength on the evaluation of the above mentioned upper limit for the NSM CFRP prestress level.

2. EXPERIMENTAL PROGRAM

2.1. Slab specimens and series of tests

The experimental program comprised thirteen one-way RC slabs that were divided in three series (series A with 5 slabs and series B and C, each one with 4 slabs). The slab dimensions and reinforcement details are illustrated in Fig. 1. The slabs had a rectangular cross section of 600 mm × 120 mm, 2600 mm total length, 2400 mm between supports and a shear span of 900 mm. The cross section´s depth of these specimens was obtained considering the ACI-318 (ACI 2011) [21] recommendation about the minimum value for the depth of a simply supported one-way RC slab ($l/20$ = 2400/20 = 120 mm, where l is the distance between supports).

For each of the abovementioned series of tests, the adopted reinforcement was designed to impose flexural failure in the slabs. The same longitudinal steel reinforcement in the compression zone (3 bars of 6 mm diameter - 3ϕ6) was provided for all tested slabs. In terms of tensile steel reinforcements, 4 bars of 8 mm diameter (4ϕ8) were adopted for the specimens of series A and B, while 4 bars of 10 mm diameter (4ϕ10) were used in the specimens of series C. For transverse reinforcement, 6 mm diameter stirrups with spacing 300 mm (ϕ6@300mm) were applied in all of the slabs of the experimental program, whose main function was to guarantee the spacing between top and bottom flexural reinforcements.

Table 1 summarizes the characteristics of the slabs of the tested series. In each series, one slab was used as a reference and the rest of slabs were strengthened with two NSM CFRP laminates that had a cross section with a thickness of 1.4 mm and a depth of 20 mm (Fig. 2a). The length of the laminates in non-prestressed strengthened slabs was 2300 mm (Fig. 3c). According to the Fig. 3d, the extremities of the prestressed laminates were not bonded to the concrete in a length of 150 mm in order to provide the same bond length adopted in the non-prestressed strengthened slabs (2300 mm).

The thickness of the concrete cover of the longitudinal tensile steel bars was 31 mm (Fig. 1). The average value of the concrete compressive strength (f_{cm}) for series A and C was 39.5 MPa, and for series B was 15 MPa. According to

Table 1, the specimens of the series A and B had a percentage of tensile flexural reinforcement (ρ_{sl}) of 0.39%, while the specimens of the series C had a ρ_{sl} = 0.62%. For all of the series of slabs the percentage of CFRP (ρ_f) was 0.085%. The prestress load that was applied in the strengthened slabs was a portion of the ultimate tensile strength of the CFRP laminates (0%, 20%, 40% and 50% prestress level in series A; 0%, 20% and 40% prestress level in series B and C).

Series A had the intent of evaluating the effect of the prestress level in NSM CFRP laminates (0%, 20%, 40% and 50%) for the flexural strengthening of one-way RC slabs of moderately high f_{cm} (39.5 MPa) and relatively low ρ_{sl} (0.39%), which is a little bit higher than the minimum ρ_{sl} according to the major part of design codes for RC structures. The efficacy of NSM technique with prestressed CFRP laminates for the flexural strengthening of low-strength concrete one-way slabs was assessed in the tests of the slabs of series B (f_{cm} = 15 MPa). In fact, the major part of the prestressed levels (0%, 20% and 40%) used in slabs of series A were also adopted in slabs of series B, and the difference between the slabs of series A and B was only the concrete strength: 15 MPa in series B and 39.5 MPa in series A. To specifically evaluate the influence of existing tensile flexural reinforcement percentage (ρ_{sl}) on the performance of prestressed NSM CFRP laminates for the flexural strengthening of one-way RC slabs, series C of tests was carried out. In this series, three of the four prestressed levels (0%, 20% and 40%) used in slabs of series A were also adopted in slabs of series C, and the difference between the slabs of series A and C was only the percentage ρ_{sl}: 0.62% in series C and 0.39% in series A.

Details about the strengthening procedures of the tested RC slabs with non-prestressed (Fig. 2b) and prestressed (Fig. 2c) NSM CFRP laminates can be found in [20].

2.2. Materials properties

The evaluation of the compressive strength and the elasticity modulus of the concrete was done when the slab tests were executed. For this purpose, direct compression tests [22-23] were carried out using cylinders with 150 mm of diameter and 300 mm of height. At the age of the test of the slabs of series A and C, the average value of the compressive strength (f_{cm}) and elasticity modulus (E_{cm}) of the concrete was, respectively, 39.5 MPa and 32.6 GPa, while the slabs of series B presented f_{cm}=15.0 MPa and E_{cm}=25.0 GPa.

Uniaxial tensile tests were carried out [24] to obtain the tensile properties of the steel bars used as internal reinforcement in the tested slabs. The average value of the yield stress of the steel bars of 6, 8, and 10 mm diameter was 528, 556 and 548 MPa, respectively, while the average value of the tensile strength for these corresponding bars was: 651, 680 and 670 MPa.

The tensile properties of the adopted CFRP laminate for this experimental program (CFK 150/2000 S&P laminates) were evaluated by uniaxial tensile tests following the recommendations of ISO 527-5 [25]. The average value of the tensile strength, elasticity modulus and ultimate strain of this CFRP laminate was 2770 MPa, 176 GPa, and 15.8‰, respectively.

To bond the NSM CFRP laminates to the concrete substrate, the S&P Resin epoxy adhesive was used. An average tensile strength of 20 MPa and an elasticity modulus of 7 GPa were determined by Costa and Barros [26] carrying out direct tensile tests according to the ISO 527-2 [27].

2.3. Test setup and monitoring system

All slab specimens were tested under four-point loading configuration (Fig. 2d and 2e), and the load was applied in displacement control mode at a rate of 1.2 mm/min. Fig. 3 shows details of the adopted instrumentation in the tested slabs: five displacement transducers (LVDT 1 to LVDT 5) were used to record the deflection of the slabs (Fig. 3a); two strain gauges (SG-S1 and SG-S2) were utilized to measure the strain on two longitudinal tensile steel bars (Fig. 3b); three strain gauges (SG-L1, SG-L2 and SG-L3) were applied on two NSM CFRP laminates to evaluate the strain evolution in the considered sections (Fig. 3c for the case of non-prestressed slabs, and Fig. 3d for the case of prestressed slabs).

3. EXPERIMENTAL RESULTS AND DISCUSSION

3.1. General behavior of one-way RC slabs flexurally strengthened with prestressed NSM CFRP laminates

Fig. 4 shows the load *vs.*mid span deflection curves for the RC slabs of the series A, B and C. Regardless of the tested series of the slabs, these curves includes three major stages: until the cracking of the concrete; between concrete cracking and yield initiation of the tensile steel reinforcement; and between tensile steel yield initiation and ultimate load. In this last stage, the non-strengthened reference slabs (A-REF, B-REF and C-REF, respectively, for series A, B and C) presented an almost plastic behavior. The third stage of the strengthened slabs' curve had almost linear behavior. This was due to linear behavior of the CFRP laminates, while steel reinforcement was yielded with concrete in its cracking stabilized phase. In fact, the load carrying capacity of the strengthened slabs has increased after the yield initiation up to the CFRP laminates' rupture, after which the load dropped to the reference slab' capacity. Regardless of the prestress level, the concrete strength and the percentage of existing steel reinforcement, the tested CFRP configuration increased the load carrying capacity of the RC slabs at service and ultimate conditions.

Table 2 displays the main results of the tested series of RC slabs in terms of cracking (F_{cr}), service (F_{serv}), yielding (F_{sy}) and maximum (F_{max}) loads. The values of the deflection at mid-span for the loads F_{sy} (u_{Fsy}) and F_{max} (u_{Fmax}) are also presented in Table 2. The service load (F_{serv}) is the load corresponding to the maximum allowed deflection for serviceability limit states (u_{Fserv}), which according to the Eurocode 2 [28] is *l/250*, where *l* is the clear length of the slab (*l*/250 = 2400 mm/250 = 9.6 mm). The yielding load is assumed the load at which a considerable decay of stiffness has occurred in the post cracking stage of a tested slab.

According to the results of the Table 2, the application of NSM CFRP laminates for the flexural strengthening of RC slabs has provided an increase of F_{cr} with the prestress level. In fact, the values of F_{cr} of non-prestressed slab (A-S0) and the average value of F_{cr} of prestressed slabs (A-S20, A-S40 and A-S50) of series A are, respectively, 1.00 and 1.87 times the value of F_{cr} of the A-REF reference slab; the values of F_{cr} of non-prestressed slab (B-S0) and the average value of F_{cr} of prestressed slabs (B-S20 and B-S40) of series B are, respectively, 1.38 and 3.97 times the value of F_{cr} of the B-REF reference slab; finally, the values of F_{cr} of non-prestressed slab (C-S0) and the average value of F_{cr} of prestressed slabs (C-S20 and C-S40) of series C are, respectively, 1.07 and 2.02 times the value of F_{cr} of the C-REF reference slab.

The obtained values for the service load (F_{serv}) of the reference (A-REF), non-prestressed (A-S0) and prestressed slabs (A-S20, A-S40 and A-S50) of series A prove the advantages of the application of prestress in the laminates. In fact, the load F_{serv} of non-prestressed slab and the average value of F_{serv} of prestressed slabs are, respectively, 1.22 and 2.12 times the load F_{serv} of the reference slab. This tendency was also verified in the slabs of series B (the value of F_{serv} of non-prestressed and the average value of F_{serv} of prestressed slabs are, respectively, 1.42 and 2.57 times the load F_{serv} of the reference slab) and series C (the values of F_{serv} of non-prestressed and the average value of F_{serv} of prestressed slabs are, respectively, 1.09 and 1.60 times the value of F_{serv} of the reference slab).

As occurred in terms of F_{cr} and F_{serv}, the yielding load (F_{sy}) has also increased with the level of prestress. In fact, the load F_{sy} of non-prestressed slab and the average value of F_{sy} of prestressed slabs of series A are, respectively, 1.41 and 2.08 times the value of F_{sy} of the A-REF reference slab; the value of F_{sy} of non-prestressed slab and the average value of F_{sy} of prestressed slabs of series B are, respectively, 1.51 and 2.04 times the value of F_{sy} of the B-REF reference slab; finally, the value of F_{sy} of non-prestressed slab and the average value of F_{sy} of prestressed slabs of series C are, respectively, 1.20 and 1.54 times the value of F_{sy} of the C-REF reference slab.

For all of the tested series, the maximum load (F_{max}) of the prestressed slabs was similar to the F_{max} of the non-prestressed slabs, since all the strengthened slabs failed by the rupture of the CFRP. The values of F_{max} of strengthened slabs ranged from 60.7 kN to 66.1 kN in series A (which is 2.10 to 2.29 times higher than the F_{max} of the reference slab of this series), from 51.1 kN to 55.7 kN in series B (which is 2.15 to 2.34 times higher than the F_{max} of the reference slab of this series), and from 69.0 kN to 71.4 kN in series C (which is 1.59 to 1.64 times higher than the F_{max} of the reference slab of this series).

Since the increase of the prestress level provided an increase of the cracking load of the slabs, but did not affect significantly the stiffness and the load amplitude between crack initiation and yield initiation, the deflection at yield initiation (u_{Fsy}) remained similar regardless of the level of prestress. In fact, the deflection u_{Fsy} of the strengthened slabs ranged from 26.6 mm to 29.1 mm in series A, from 31.5 mm to 32.0 mm in series B, and from 30.5 mm to 31.5 mm in series C. As the initial strains in the CFRP laminates increased with prestress level, and considering that the strengthened slabs failed by the tensile rupture of the CFRP, the slab's deflection at maximum load (u_{Fmax}) has decreased with the prestress level (the values of u_{Fmax} in the non-prestressed, 20%, 40% and 50% prestressed slabs of series A are, respectively, 89.8 mm, 65.4 mm, 50.3 mm and 42.5 mm; the values of u_{Fmax} in the non-prestressed, 20% and 40% prestressed slabs of series B are, respectively, 102.9 mm, 78.2 mm and 58.8 mm; and 92.8 mm, 71.2 mm and 51.3 mm for non-prestressed, 20% and 40% prestressed slabs of series C).

3.2. Crack pattern, failure modes and strains in CFRP laminates

In all tested slabs, the first cracks occurred in the pure bending zone (between the loaded sections). In the subsequent loading process, the cracks became wider and new cracks started to initiate in the shear spans of the slabs. The crack pattern of the slabs of series A (A-REF, A-S0, A-S20, AS-40 and AS-50) at the end of the test is represented in Fig. 5, where it is possible to see that the average distance between cracks (d_{cr}) measured in the tension face of the RC slabs has decreased with the level of prestress (the values of d_{cr} are 145 mm, 89 mm, 87.7 mm, 83 mm and 80 mm for the slabs, respectively, A-REF, A-S0, A-S20, A-S40 and A-S50). For series B, the values of d_{cr} are 126 mm, 101 mm, 86 mm and 79 mm in slabs, respectively, B-REF, B-S0, B-S20 and B-S40. For series C, the values of d_{cr} are 111 mm, 86 mm, 84 mm and 84 mm for the slabs, respectively, C-REF, C-S0, C-S20 and C-S40. The analysis of the cracking process of the tested slabs up to their failure has shown that the use of NSM technique with CFRP laminates as a flexural strengthening leads to a decrease of the cracks' widths. Furthermore, due to the initial compressive strain field applied by the prestress, the length of the slab's cracked band ($l_{cr,band}$) has decreased with the increase of the level of prestress (Fig. 5): the values of $l_{cr,band}$ in series A are 1452 mm, 1779 mm, 1579 mm, 1333 mm and 1284 mm for the slabs, respectively, A-REF, A-S0, A-S20, A-S40 and A-S50; in series B are 1639 mm, 1826 mm, 1550 mm and 1260 mm for the slabs, respectively, B-REF, B-S0, B-S20 and B-S40; and in series C are 1776 mm, 1892 mm, 1681 mm and 1554 mm for the slabs, respectively, C-REF, C-S0, C-S20 and C-S40.

Regardless of the tested series (A, B and C), the failure mode of the reference slabs without CFRP occurred by the concrete crushing after the yielding of the tensile steel reinforcements (Fig. 6a). In slabs A-REF, B-REF and C-REF, a longitudinal steel bar has ruptured at a mid-span deflection of 107 mm, 143 mm and 119 mm, respectively (Fig. 4). All of the tested CFRP strengthened slabs failed by the rupture of the laminates after the yielding of the tensile steel reinforcements (Fig. 6b).

In the column "Total" of Table 3 is indicated the maximum values of strain recorded up to the maximum load (F_{max}) in the strain gauges applied to the CFRP laminates of the slabs. These values were obtained adding the strain at the end of the prestressing process (column "Prestressing") to the maximum strain registered during the four point bending test up to F_{max} (column "Test"). It can be observed in Table 3 that the maximum CFRP strain values (column "Total") was recorded in SG-L1 (A-S0, A-S40, C-S0 and C-S40) and SG-L2 (slabs A-S20, A-S50, BS-0, B-S20, B-S40 and C-S20), both positioned in the pure bending zone (between the load sections). The average value of the maximum CFRP strain for the tested slabs was 15.4‰ which corresponds to 98% of its ultimate strain, therefore justifying the failure mode of tested CFRP strengthened slabs and the high performance of the NSM technique with CFRP laminates for the flexural strengthening of one-way RC slabs.

3.3. Effect of the prestress level on the performance of prestressed NSM CFRP laminates

To assess the influence of the CFRP prestress level on the general behavior of the slabs, the values of loads (F_{cr}^{Str}, F_{serv}^{Str}, F_{sy}^{Str} and F_{max}^{Str}) and corresponding deflection to F_{max}^{Str} ($u_{F_{max}}^{Str}$) of the strengthened prestressed slabs of series A were compared with those corresponding values of the reference slab (F_{cr}^{Ref}, F_{serv}^{Ref}, F_{sy}^{Ref} and F_{max}^{Ref} and $u_{F_{max}}^{Ref}$). By considering these values, the parameters $\Delta F_{cr}/F_{cr}^{Ref}$, $\Delta F_{serv}/F_{serv}^{Ref}$, $\Delta F_{sy}/F_{sy}^{Ref}$, $\Delta F_{max}/F_{max}^{Ref}$ and $\Delta u_{F_{max}}/u_{F_{max}}^{Ref}$ were evaluated and included in Table 4, where $\Delta F_{cr} = F_{cr}^{Str} - F_{cr}^{Ref}$, $\Delta F_{serv} = F_{serv}^{Str} - F_{serv}^{Ref}$, $\Delta F_{sy} = F_{sy}^{Str} - F_{sy}^{Ref}$, $\Delta F_{max} = F_{max}^{Str} - F_{max}^{Ref}$ and $\Delta u_{F_{max}} = u_{F_{max}}^{Str} - u_{F_{max}}^{Ref}$.

According the results of Table 4, a CFRP prestress level of 0%, 20%, 40% and 50% has provided an increase of, respectively, 0%, 38.8%, 98.3% and 122.3% in cracking load, an increase of, respectively, 21.7%, 76.3%, 121.7% and 136.8% in service load, an increase of, respectively, 40.9%, 89.9%, 113.8% and 119.4% in yielding load, and an increase of, respectively, 110.0%, 128.7%, 128.4% and 120.4% in maximum load. The obtained results show that the maximum deflection has increased in 10.8% for the prestress level of 0%, while it has decreased in 19.3%, 37.9% and

47.5% by applying a prestress level of, respectively, 20%, 40% and 50%. Nonetheless, the level of ductility is still very high in all prestressed slabs since at u_{Fmax} it was verified a significant plastic incursion in the steel reinforcement.

Fig. 7a shows the effect of increasing the prestressing level on the cracking, service, yielding, and ultimate loads with respect to the A-REF reference slab and the non-prestressed strengthened slab A-S0. According to this figure, by increasing the prestressing levels significantly increased the cracking, service and yielding loads, but had almost no effect on the maximum loads (all of the strengthened slabs failed by the rupture of the CFRP). Fig. 7b represents the effect of increasing the prestress level on the deflection at yielding and ultimate loads, where it is possible to conclude that existed a significant decrease of the deflection at ultimate load with the increase of the prestress level, but the deflection at yield was not considerably affected by the prestress level.

Fig. 8a displays the relationship between the level of prestress and the normalized value of energy consumed during the loading of the RC slabs of series A. For this purpose, the energy consumed was evaluated for each slab as the area under the load-deflection curve up to the u_{Fmax} and the normalized value of energy was calculated for the following two cases: the ratio between the energy of the strengthened slab and the energy of the reference slab (A-REF), and the ratio between the energy of the prestressed strengthened slab and the energy of the non-prestressed strengthened slab (A-S0). In both cases, by increasing the level of prestress, the normalized absorption energy decreased almost linearly.

To assess the ductility performance of the slabs, the ductility index μ was evaluated, which is defined as the ratio between deflection at mid-span for F_{max} (u_{Fmax}) and deflection at mid-span for yield initiation (u_{Fsy}) of the slab ($\mu = u_{Fmax}/u_{Fsy}$). Fig. 8b displays, for the strengthened slabs of series A, the relation between the normalized ductility index (ratio between the ductility index of the prestressed strengthened slab and the ductility index of the non-prestressed strengthened slab) and the prestress level. Based on Fig. 8b, by increasing the prestress level, the normalized ductility index decreased almost linearly.

3.4. Effect of the concrete strength on the performance of prestressed NSM CFRP laminates

The effect of the concrete strength on the performance of the prestressed NSM CFRP laminates was analyzed by the comparison of the obtained results in series A and B (the difference between the slabs of series A and B was only the concrete compressive strength: f_{cm} = 15 MPa in series B and f_{cm} = 39.5 MPa in series A). For both series, Table 5 shows the obtained values for the parameters $\Delta F_{cr}/F_{cr}^{Ref}$, $\Delta F_{serv}/F_{serv}^{Ref}$, $\Delta F_{sy}/F_{sy}^{Ref}$, $\Delta F_{max}/F_{max}^{Ref}$ and $\Delta u_{F_{max}}/u_{F_{max}}^{S0}$.

According to the results of Table 5, the application of a CFRP prestress level of 20% in the slabs with higher (series A) and lower (series B) values of f_{cm} increased the cracking load by 39% and 223%, respectively, while 40% prestress level provided an increase of 98% and 372%, respectively. By applying 20% of prestress in RC slabs with f_{cm} = 39.5 MPa (series A) and f_{cm} = 15 MPa (series B), the service load has increased, respectively, 76% and 123%, while 40% prestress level provided an increase of 122% and 190%, respectively. The increment of yielding load of prestressed slabs was almost the same regardless the concrete quality (about 90% and 114%-118%, respectively, for 20% and 40% prestress levels). The application of a CFRP prestress level of 20% in the slabs with higher (series A) and lower (series B) value of f_{cm} increased the ultimate load by 129% and 124%, respectively, while 40% prestress level provided an increase of 128% and 134%, respectively. The decrease of the ultimate deflection of prestressed slabs (compared to the corresponding values of slabs without prestress) was almost the same regardless of the concrete strength (24%-27% and 43%-44%, respectively, for 20% and 40% prestress levels).

Fig. 9a, 9b and 9c shows that, regardless of the concrete strength, by increasing the level of prestress in the NSM laminates, the load carrying capacity of RC slabs at cracking, service and yielding has improved. The influence of the level of prestress for the increase of the cracking and service loads was more noticeable in the slabs with lower value of f_{cm}. By increasing the level of prestress, the increase of the yielding and the ultimate load carrying capacity of the slabs with different concrete compressive strength was almost the same (Fig. 9c and 9d). Increasing the prestress level decreased the deflection at the maximum load and the decrement was almost the same in both concrete strength class (Fig. 9e). Therefore the strength of the concrete had almost no effect on the maximum loads since the failure mode of all of the strengthened slabs was governed by the rupture of the CFRP.

3.5. Effect of the percentage of tensile reinforcement on the performance of prestressed NSM CFRP laminates

The effect of the percentage of the longitudinal reinforcement (ρ_{sl}) on the performance of the prestressed NSM CFRP laminates was analyzed by comparing the obtained results in series A and C (the difference between the slabs of series A and C was the amount of the tensile longitudinal reinforcement: 4ϕ8 in series A that corresponds to ρ_{sl} = 0.39%, and 4ϕ10 in series C that corresponds to ρ_{sl} = 0.62%. For both series, Table 6 shows the obtained values for the parameters $\Delta F_{cr}/F_{cr}^{Ref}$, $\Delta F_{serv}/F_{serv}^{Ref}$, $\Delta F_{sy}/F_{sy}^{Ref}$, $\Delta F_{max}/F_{max}^{Ref}$ and $\Delta u_{F_{max}}/u_{F_{max}}^{S0}$.

According to the results of Table 6, the application of a CFRP prestress level of 20% in the slabs with lower (series A) and higher (series C) values of ρ_{sl} increased the cracking load by 39% and 75%, respectively, while 40% prestress level provided an increase of 98% and 129%, respectively. By applying 20% of prestress in RC slabs with ρ_{sl} = 0.39%

(series A) and ρ_{sl} = 0.62% (series C), the service load has increased, respectively, 76% and 42%, while 40% prestress level provided an increase of 122% and 79%, respectively. By applying 20% of prestress in RC slabs with lower and higher percentage of flexural reinforcement, the yielding load has increased, respectively, 90% and 40%, while 40% of prestress provided an increase of 114% and 68%, respectively.

The application of a CFRP prestress level of 20% in the slabs with lower (series A) and higher (series C) value of ρ_{sl} increased the ultimate load by 129% and 59%, respectively, while 40% prestress level provided an increase of 129% and 64%, respectively. The decrease of the ultimate deflection of prestressed slabs with lower and higher percentage of flexural reinforcement was, respectively, 27% and 23%, by applying 20% of prestress, while 40% of prestress has provided a decrease of 44% and 45%.

Fig. 10a, 10b and 10c shows that, regardless of the percentage of the flexural reinforcement, by increasing the level of prestress in the NSM laminates, the load carrying capacity of RC slabs in cracking, service and yielding has increased. The influence of the level of prestress for the increase of the service and yielding loads was more noticeable in the slabs with lower percentage of flexural reinforcement, and this effect for increasing the cracking loads was more noticeable in the slabs with higher percentage of flexural reinforcement. With the increase of the prestress level, the ultimate load of the slabs has not changed significantly regardless of the percentage of flexural reinforcement (Fig. 10d), and the deflection corresponding to maximum load has decreased (Fig. 10e). Regardless of the level of prestress, with the decrease of the percentage of flexural reinforcement, the ultimate load of the RC slabs has increased more significantly than the reference slab.

4. ANALYTICAL APPROACH

An analytical approach was developed to predict the cracking, yielding and maximum loads of RC slabs flexurally strengthened with prestressed NSM CFRP laminates. Then, the predictive performance of this analytical formulation was appraised by comparing the analytical and experimental results. Furthermore, an upper limit for the prestress level was proposed for ensuring a compromise of ductility and strengthening effectiveness of the prestressed strengthened slabs. Additionally, a parametric study was also executed to highlight the influence of the percentage of tensile flexural reinforcement and the concrete strength on the evaluation of the upper limit for the NSM CFRP prestress level.

4.1. Cracking, yielding and maximum loads

The effect of the loads that will be on the RC structural member during the installation of the CFRP system (initial strain level) should be considered in the calculation of the RC strengthened member load carrying capacity. In fact, the initial strain level was considered in the developed analytical formulation, namely the following strains: in the concrete on the bottom fiber of the cross section (ε_{cr0}); in the concrete at the level of the centroid of the NSM CFRP laminates (ε_{bi}); in the longitudinal bottom steel bars (ε_{s0}); in the concrete on the top fiber of the cross section (ε_{c0}).

For the case of a cross section flexurally strengthened with prestressed NSM CFRP laminates, two different cases should be considered for the initial strain level (case I and case II). In case I, it is supposed that the concrete top fiber is in compression and the concrete bottom fiber is in tension (the moment due to the loads that will be on the RC slab during the installation of the CFRP system is positive). In case II, the top and bottom fibers are considered in tension and compression, respectively (the moment due to the loads that will be on the RC slab during the installation of the CFRP system is negative).

4.1.1. Bending moment at crack initiation

The strain and stress distribution along the height of slab's cross section and the balance of internal forces corresponding to the crack initiation state are indicated in Fig. 11. The strain compatibility between constituent materials allows to obtain the strain in these materials from the concrete cracking tensile strain, ε_{cr}, first occurred in the concrete bottom surface (corresponding to the mean value of the axial tensile strength of the concrete, f_{ctm} [28]), by using Eqs. (1) to (4). Taking into account the internal force equilibrium of the cross section, Eq. (5) is obtained.

$$\varepsilon_c = (\varepsilon_{cr} \pm \varepsilon_{cr0}).\, c_{cr}/(h - c_{cr}) \tag{1}$$

$$\varepsilon_{f,cr} = (\varepsilon_{cr} \pm \varepsilon_{cr0}).\frac{d_f - c_{cr}}{h - c_{cr}} - \varepsilon_{bi} \tag{2}$$

$$\varepsilon_s = (\varepsilon_{cr} \pm \varepsilon_{cr0}).\,(d_s - c_{cr})/(h - c_{cr}) \tag{3}$$

$$\varepsilon'_s = (\varepsilon_{cr} \pm \varepsilon_{cr0}).\,(c_{cr} - d'_s)/(h - c_{cr}) \tag{4}$$

$$F_c + F'_s = F_{cr} + F_s + F_f \;\rightarrow\; \frac{E_c.\varepsilon_c.b.c_{cr}}{2} + A'_s.E_s.\varepsilon'_s = E_c.(\varepsilon_{cr} \pm \varepsilon_{cr0}).b.(h - c_{cr})/2 + A_s.E_s.\varepsilon_s + A_f.E_f.\left(\varepsilon_p + \varepsilon_{f,cr}\right) \tag{5}$$

In the above mentioned equations the adopted symbols have the following meaning (Fig. 11): b and h are the width and height of the cross section of the RC slab, respectively; d'_s, d_s and d_f are the effective depth of the longitudinal top and bottom steel bars and CFRP laminates, respectively; c_{cr} is the distance from extreme compression fiber to the neutral axis; E_c, E_s and E_f are the modulus of elasticity of the concrete, steel and CFRP, respectively; A'_s, A_s, and A_f are the cross sectional area of the longitudinal top and bottom steel bars and CFRP laminates, respectively; ε_p is the initial prestress strain in the CFRP laminates; ε_c and ε'_s are the compressive strain of the concrete top fiber and longitudinal top steel bars, respectively; ε_s and $\varepsilon_{f,cr}$ are the tensile strain of the longitudinal bottom steel bars and CFRP laminates, respectively.

By substituting Eqs. (1) to (4) into (5), the neutral axis depth c_{cr} can be determined with Eq. (6). The bending moment corresponding to the crack initiation is determined by adding the internal moments produced by the forces in relation to the neutral axis of the cross section (Eq. (7)).

$$c_{cr} = \frac{E_s.(A'_s.d'_s + A_s.d_s) + A_f.E_f.(d_f + \frac{\varepsilon_p - \varepsilon_{bi}}{\varepsilon_{cr} \pm \varepsilon_{cr0}}.h) + 0.5b.h^2.E_c}{E_s.(A'_s + A_s) + A_f.E_f.\left(1 + \frac{\varepsilon_p - \varepsilon_{bi}}{\varepsilon_{cr} \pm \varepsilon_{cr0}}\right) + b.h.E_c} \quad (6)$$

$$M_{cr} = A'_s.E_s.\varepsilon'_s.(c_{cr} - d'_s) + E_c.\varepsilon_c.b.\frac{c_{cr}^2}{3} + E_c.b.(\varepsilon_{cr} \pm \varepsilon_{cr0}).(h - c_{cr})^2/3 + A_s.E_s.\varepsilon_s.(d_s - c_{cr}) + A_f.E_f.(\varepsilon_p + \varepsilon_{f,cr}).(d_f - c_{cr}) \quad (7)$$

In "±" of Eqs. (1) to (7), the negative sign should be adopted for the case I of the initial strain level (positive moment due to the loads that will be on the RC slab during the installation of the CFRP), while the positive sign should be adopted for the case II of the initial strain level (negative moment due to the loads that will be on the RC slab during the installation of the CFRP). Moreover for the case I, ε_{bi}=0 should be considered in the Eqs. (2) and (6).

4.1.2. Bending moment at yield initiation

To determine the bending moment corresponding to the yield initiation, some simplifications in relation to the previous adopted approach are assumed. In fact, the contribution of the concrete in tension for the resisting bending moment at yield initiation is neglected, and the strain profile for the concrete in compression is assumed to be linear (Fig. 12). Eqs. (8) to (10) present the geometric relationships between strains along the height of the cross section as a function of the steel yield initiation strain, ε_{sy}, while Eq. (11) represents the internal force equilibrium of the cross section.

$$\varepsilon_c = (\varepsilon_{sy} \pm \varepsilon_{s0}).c_{sy}/(d_s - c_{sy}) \quad (8)$$

$$\varepsilon_{f,sy} = (\varepsilon_{sy} \pm \varepsilon_{s0}).\frac{d_f - c_{sy}}{d_s - c_{sy}} - \varepsilon_{bi} \quad (9)$$

$$\varepsilon'_s = (\varepsilon_{sy} \pm \varepsilon_{s0}).(c_{sy} - d'_s)/(d_s - c_{sy}) \quad (10)$$

$$F_c + F'_s = F_{sy} + F_f \;\rightarrow\; \frac{E_c.\varepsilon_c.b.c_{sy}}{2} + A'_s.E_s.\varepsilon'_s = A_s.E_s.(\varepsilon_{sy} \pm \varepsilon_{s0}) + A_f.E_f.(\varepsilon_p + \varepsilon_{f,sy}) \quad (11)$$

In Fig. 12 and Eq. (11), f_{sy} and $\varepsilon_{f,sy}$ are, respectively, the steel stress and the tensile strain of the CFRP laminates, both at steel yield initiation. By substituting Eqs. (8) to (10) into Eq. (11), the neutral axis depth c_{sy} can be determined with Eq. (12). The bending moment corresponding to the steel yield initiation is obtained by adding the internal moments produced by the force components in relation to the neutral axis of the cross section (Eq. (13)).

$$[b.E_c/2].{c_{sy}}^2+\left[A'_s.E_s+A_s.E_s+A_f.E_f.(1+\frac{\varepsilon_p-\varepsilon_{bi}}{\varepsilon_{sy}\pm\varepsilon_{s0}})\right].c_{sy} - \left[A'_s.E_s.d'_s+A_s.E_s.d_s+A_f.E_f.(d_f+d_s.\frac{\varepsilon_p-\varepsilon_{bi}}{\varepsilon_{sy}\pm\varepsilon_{s0}})\right]=0 \tag{12}$$

$$M_{sy}=A'_s.E_s.\varepsilon'_s.\left(c_{sy}-d'_s\right)+E_c.\varepsilon_c.b.c_{sy}^2/3+A_s.E_s.(\varepsilon_{sy}\pm\varepsilon_{s0}).(d_s-c_{sy})+A_f.E_f.\left(\varepsilon_p+\varepsilon_{f,sy}\right).(d_f-c_{sy}) \tag{13}$$

In "±" of Eqs. (8) to (13), the negative and positive sign should be adopted, respectively, for the case I and case II of the initial strain level. Moreover for the case I, ε_{bi}=0 should be considered in the Eqs. (9) and (12).

4.1.3. Maximum bending moment

The experimental studies evidenced that the prevalent failure mode of the prestressed RC slabs is the rupture of the CFRP laminate due to the attainment of its ultimate tensile strain ε_{fu} ($\varepsilon_{fu}=\varepsilon_p+\varepsilon_{fb}$, where ε_p is the initial strain due the prestress process and ε_{fb} is the subsequent tensile strain caused by the four point bending test (bending moment) (Fig. 13)). In this context, an equation was developed to obtain the neutral axis depth c_{fu} of the cross section at the ultimate stage considering the strain in the CFRP laminate be equal to ε_{fu}.

The distribution of strain and stress along the height of slab's cross section and the balance of internal forces corresponding to the ultimate state (Fig. 13) are based on ACI 440.2R-08 recommendations [29]. Taking into account the internal force equilibrium of the cross section, it is obtained Eq. (14).

$$\pm F_{c2}+F_{c1}+F'_s=F_{sy}+F_{fu}\ \rightarrow\ \pm\frac{E_c.\varepsilon_{c0}.b.c_{fu}}{2}+\alpha_1.f'_c.\beta_1.c_{fu}.b+A'_s.\varepsilon'_s.E_s = A_s.E_s.(\varepsilon_{sy}\pm\varepsilon_{s0}).+A_f.E_f.(\varepsilon_p+\varepsilon_{fb}) \tag{14}$$

In Eq. (14), f'_c is the concrete compressive strength and α_1 and β_1 are parameters to define the rectangular compression stress block in the concrete (Fig. 13). Eqs. (15) to (20) present the parameters α_1 and β_1 and the geometric relationships between strains along the height of cross section (c_{fu} is the distance from extreme compression fiber to the neutral axis when the CFRP rupture is the governing failure mode; ε'_c is the strain at f'_c). The geometric relationships between strains (Eqs. (18) and (19)) are presented as a function of the tensile strain of the CFRP laminate caused by sum of the bending moment (ε_{fb}) and the initial strain (ε_{bi}).

$$\beta_1=(4\varepsilon'_c-\varepsilon_c)/(6\varepsilon'_c-2\varepsilon_c) \tag{15}$$

$$\alpha_1=(3\varepsilon'_c.\varepsilon_c-\varepsilon_c^2)/(3\varepsilon_c'^2.\beta_1) \tag{16}$$

$$\varepsilon_c' = 1.7 f_c'/E_c \tag{17}$$

$$\varepsilon_c = (\varepsilon_{fb} + \varepsilon_{bi}).\, c_{fu}/(d_f - c_{fu}) \tag{18}$$

$$\varepsilon_s' = (\varepsilon_{fb} + \varepsilon_{bi}).\, (c_{fu} - d_s')/(d_f - c_{fu}) \tag{19}$$

$$\varepsilon_{fb} = \varepsilon_{fu} - \varepsilon_p \tag{20}$$

Substituting Eqs. (15) to (20) into Eq. (14) leads to Eq. (21), whose resolution provides the neutral axis depth at ultimate stage:

$$A.\, {c_{fu}}^3 + B.\, {c_{fu}}^2 + C.\, c_{fu} + D = 0 \tag{21}$$

$$A = (\varepsilon_{fb} + \varepsilon_{bi}).\, f_c'.\, b.\, \left(3\varepsilon_c' + \varepsilon_{fb} + \varepsilon_{bi}\right) \mp 1.5\varepsilon_c'^2.\, E_c.\, \varepsilon_{c0}.\, b \tag{21a}$$

$$B = 3.\, \varepsilon_c'.\, \left[(\varepsilon_{fb} + \varepsilon_{bi}).\, \varepsilon_c'.\, E_s.\, A_s' - (\varepsilon_{fb} + \varepsilon_{bi}).\, f_c'.\, b.\, d_f + \varepsilon_c'.\, \left(A_f.\, E_f.\, \varepsilon_{fu} + A_s.\, E_s.\, (\varepsilon_{sy} \pm \varepsilon_{s0})\right) \pm \varepsilon_c'.\, E_c.\, \varepsilon_{c0}.\, b.\, d_f\right] \tag{21b}$$

$$C = -3\varepsilon_c'^2.\, \left[(\varepsilon_{fb} + \varepsilon_{bi}).\, E_s.\, A_s'.\, \left(d_f + d_s'\right) + 2d_f.\, (A_f.\, E_f.\, \varepsilon_{fu} + A_s.\, E_s.\, (\varepsilon_{sy} \pm \varepsilon_{s0})) \pm 0.5 d_f^2.\, E_c.\, \varepsilon_{c0}.\, b\right] \qquad \text{21c)}$$

$$D = 3\varepsilon_c'^2.\, d_f.\, \left[(\varepsilon_{fb} + \varepsilon_{bi}).\, E_s.\, A_s'.\, d_s' + d_f.\, (A_f.\, E_f.\, \varepsilon_{fu} + A_s.\, E_s.\, (\varepsilon_{sy} \pm \varepsilon_{s0}))\right] \tag{21d}$$

For the case I, ε_{bi}=0 should be considered in the Eqs. (19), (21c), (21d) and first term of Eq. (21b) while for the case II, ε_{bi}=0 should be considered in the Eqs. (18), (21a) and second term of Eq. (21b).

If Eq. (21) doesn't have real root then failure will be due to the concrete crushing. In this case, the neutral axis depth should be evaluated considering the ultimate compressive strain for the concrete top fiber. The geometric relationships between strains (Eqs. (22) and (23)) are presented as a function of the ultimate compressive strain of the concrete (ε_{cu}). Substituting Eqs. (22) and (23) into Eq. (14) (with substituting c_{fu} to c_{cu} in Eq. (14)) with considering α_1=0.85 and β_1 based on ACI 318-05 recommendations for concrete crushing failure mode leads to Eq. (24), whose resolution provides the neutral axis depth at ultimate stage:

$$\varepsilon_s' = (\varepsilon_{cu} \pm \varepsilon_{c0}).\, (c_{cu} - d_s')/c_{cu} \tag{22}$$

$$\varepsilon_{fb} = (\varepsilon_{cu} \pm \varepsilon_{c0}).\, \frac{d_f - c_{cu}}{c_{cu}} - \varepsilon_{bi} \tag{23}$$

$$(\pm 0.5 E_c.\, \varepsilon_{c0}.\, b + \alpha_1.\, f_c'.\, \beta_1.\, b).\, {c_{cu}}^2 + \left[A_s'.\, E_s.\, (\varepsilon_{cu} \pm \varepsilon_{c0}) - A_s.\, E_s.\, (\varepsilon_{sy} \pm \varepsilon_{s0}) + A_f.\, E_f.\, \left(\varepsilon_{cu} \pm \varepsilon_{c0} + \varepsilon_{bi}\right)\right].\, c_{cu} - (\varepsilon_{cu} \pm \varepsilon_{c0}).\, (A_s'.\, E_s.\, d_s' + A_f.\, E_f.\, d_f) = 0 \tag{24}$$

The maximum bending moment corresponding to the failure condition is determined by adding the internal moments produced by the force components (Eq. (25)).

$$M_{max} = A'_s . E_s . \varepsilon'_s . (c_{xu} - d'_s) \pm E_c . \varepsilon_{c0} . b . \frac{c_{xu}^2}{3} + \alpha_1 . f'_c . \beta_1 . b . {c_{xu}}^2 . \left(1 - \frac{\beta_1}{2}\right) + A_s . E_s . (\varepsilon_{sy} \pm \varepsilon_{s0}) . (d_s - c_{xu}) + A_f . E_f . (\varepsilon_{fb} + \varepsilon_p) . (d_f - c_{xu}) \quad (25)$$

In the Eq. (25), the c_{xu} will be equal to c_{fu} in the case of CFRP rupture failure mode, and will be equal to c_{cu} in the case of concrete crushing failure. The values of α_1 and β_1 should be considered related to each failure modes. For the case I, ε_{bi} =0 should be considered in the Eqs. (23) and (24), In "±" of Eqs. (14), (21b), (21c), (21d), (22), (23), (24) and (25), the negative and positive sign should be adopted, respectively, for the case I and case II of the initial strain level. In "∓" of Eq. (21a), the positive and negative sign should be adopted, respectively, for the case I and case II of the initial strain level.

4.1.4. Experimental vs. analytical results in terms of cracking, yielding and failure conditions

The analytical values of the cracking ($F_{cr,Anal}$), yielding ($F_{sy,Anal}$) and maximum ($F_{max,Anal}$) load of the prestressed slabs of the experimental program described in section 2 are calculated considering, respectively, the analytical values of the cracking ($M_{cr,Anal}$ obtained using Eq. (7)), yielding ($M_{sy,Anal}$ determined by Eq. (13)) and maximum ($M_{max,Anal}$ obtained using Eq. (25)) resisting bending moment ($F_{cr,Anal}$ = $M_{cr,Anal}$/0.45, $F_{sy,Anal}$ = $M_{sy,Anal}$/0.45 and $F_{max,Anal}$ = $M_{max,Anal}$/0.45, see Fig. 1). The comparison of the analytical values with the experimental ones ($F_{cr,exp}$, $F_{sy,exp}$ and $F_{max,exp}$) are indicated in Table 7.

The analytical values were obtained using the average values of the material properties that are presented in section 2.2 (for the elasticity modulus of the steel it was adopted E_s = 200 GPa). The average (λ_p) and coefficient of variation (V_p) of the ratio between experimental and analytical values for the stages corresponding to crack initiation, steel yield initiation and failure conditions are also indicated in Table 7. Considering the use of the average values of the material properties for the calculation of the analytical values, the ratio between experimental and analytical values higher than 1.0 is synonymous of safety condition. The results obtained evidence that the analytical method is quite accurate since, for the three analyzed scenarios, the average value (λ_p) varied between 1.11 to 1.18, and the coefficient of variation (V_p) varied between 6% to 26% (the slab B-S0, in terms of the cracking load, was not considered in this analysis due an abnormal value of the ratio $F_{cr,exp}$/ $F_{cr,Anal}$). According to the results of Table 7, the analytical approach provides safe results for all of the prestressed RC slabs in the case of yielding and maximum load.

Figs. 14a, 14c and 14e compare the experimental and analytical values in terms of cracking (F_{cr}), yielding (F_{sy}) and maximum (F_{max}) loads for the RC slabs of the three series of tests (A, B and C), being visible the very good predictive performance for the three groups of tested slabs in special for the loads F_{sy} and F_{max}. Figs. 14b, 14d and 14f show the above mentioned relationship in terms of the level of prestress, indicating that the level of predictive performance is similar for the considered prestress levels.

4.2. Allowable maximum prestress level

Based on the obtained experimental results, the use of NSM technique with prestressed CFRP laminates for the flexural strengthening of RC slabs reduces the ductility of the original structural member. According to ACI 440.2R-08 [29] recommendations, to maintain a sufficient degree of ductility, the strain level in the steel reinforcements at the ultimate limit state (concrete crushing or tensile failure of the FRP) should be at least 0.005. Therefore to guarantee an acceptable degree of ductility for the RC slabs flexurally strengthened with prestressed NSM CFRP laminates, the highest level of prestress in the CFRP laminates should be limited in order to allow the development of tensile strain in the flexural reinforcement higher or equal to 0.005 at the ultimate stage.

4.2.1. Analytical formulation

A criterion that considers the strain compatibility between constituent materials and the principles of static equilibrium at ultimate limit condition for the flexural capacity of RC slabs strengthened with prestressed NSM CFRP laminates is herein proposed for determining the upper limit for the prestress level that assures a compromise in terms of ductility and strengthening effectiveness for this type of structural elements.

The governing failure mode in the present analytical approach is the CFRP rupture due to the attainment of its ultimate tensile strain. The allowable prestress level in the CFRP laminate is considered as:

$$\varepsilon_p = \varepsilon_{fu} - \varepsilon_{fb} \tag{26}$$

4.2.1.1. Prestress level with sufficient degree of ductility (ε_s= 0.005 ≥ ε_{sy})

The distribution of strain and the internal force equilibrium of the cross section in RC slabs are assumed those represented in Fig. 15. The internal force equilibrium is according to ACI 440.2R-08 [29] approach, by assuming a tensile strain of 0.005 in the longitudinal steel bars (ε_s= 0.005 ≥ ε_{sy}) when the rupture of the CFRP laminate occurs.

The internal force equilibrium of the cross section is provided by Eq. (14), with β_1, α_1 and ε'_c obtained from Eqs. (15) to (17). Eqs. (27) and (28) present the geometric relationships between strains along the height of cross section as a function of steel strain, $\varepsilon_s = 0.005$.

$$\varepsilon_c = 0.005.c_{sd}/(d_s - c_{sd}) \tag{27}$$

$$\varepsilon_s' = (0.005 \pm \varepsilon_{s0}).(c_{sd} - d_s')/(d_s - c_{sd}) \tag{28}$$

Substituting Eqs. (15) to (17), (27) and (28) into Eq. (14) (with substituting c_{fu} to c_{sd} in Eq. (14)) leads to Eq. (29) that determines the neutral axis c_{sd}.

$$[0.005.f_c'.b.(3\varepsilon_c' + 0.005) \mp 1.5\varepsilon_c'^2.E_c.\varepsilon_{c0}.b)].c_{sd}{}^3 + 3\varepsilon_c'.\left[(0.005 \pm \varepsilon_{s0}).\varepsilon_c'.E_s.A_s' - 0.005.f_c'.b.d_s + \varepsilon_c'.\left(A_f.E_f.\varepsilon_{fu} + A_s.E_s.(\varepsilon_{sy} \pm \varepsilon_{s0})\right) \pm \varepsilon_c'.E_c.\varepsilon_{c0}.b.d_s\right].c_{sd}{}^2 - 3\varepsilon_c'^2.\left[(0.005 \pm \varepsilon_{s0}).E_s.A_s'.(d_s + d_s') + 2d_s.(A_f.E_f.\varepsilon_{fu} + A_s.E_s.(\varepsilon_{sy} \pm \varepsilon_{s0})) \pm 0.5d_s^2.E_c.\varepsilon_{c0}.b\right].c_{sd} + 3\varepsilon_c'^2.d_s.\left[(0.005 \pm \varepsilon_{s0}).E_s.A_s'.d_s' + d_s.(A_f.E_f.\varepsilon_{fu} + A_s.E_s.(\varepsilon_{sy} \pm \varepsilon_{s0}))\right] = 0 \tag{29}$$

The maximum prestress strain that can be applied to the CFRP laminate with a sufficient degree of ductility in prestressed strengthened RC slabs is determined by:

$$\varepsilon_{fb} = \frac{0.005.(d_f - c_{sd})}{d_s - c_{sd}} - \varepsilon_{bi} \ \rightarrow \varepsilon_{p1} = \varepsilon_{fu} - \varepsilon_{fb} \tag{30}$$

Either the obtained concrete compressive strain (ε_c) exceed the ultimate compressive strain in the concrete (ε_{cu}) or Eq. (29) doesn't have positive real root then failure will be due to the concrete crushing. In this case, the neutral axis depth should be evaluated considering the ultimate compressive strain for the concrete top fiber and tensile strain equal to 0.005 for the steel reinforcement, and then the neutral axis depth c_{cu} and the maximum prestress strain are determined from:

$$c_{cu} = d_s.\varepsilon_{cu}/(0.005 + \varepsilon_{cu}) \ \rightarrow \varepsilon_{fb} = \frac{0.005.(d_f - c_{cu})}{d_s - c_{cu}} - \varepsilon_{bi} \ \rightarrow \varepsilon_{p1} = \varepsilon_{fu} - \varepsilon_{fb} \tag{31}$$

For the case II, ε_{bi}=0 should be considered in the Eqs. (30) and (31). In "±" of Eqs. (27) to (31), the negative and positive sign should be adopted, respectively, for the case I and case II of the initial strain level. In "∓" of Eq. (29), the positive and negative sign should be adopted, respectively, for the case I and case II of the initial strain level.

4.2.1.2. Maximum prestress level without concrete cracking

After releasing the prestressing load, an upward deflection is applied to the RC slab due to the eccentricity ($e=d_f-h/2$) of the prestressing load (F_p). In Eqs. (32) and (33), P_r is the applied CFRP prestress level.

$$P_r = \frac{\varepsilon_p}{\varepsilon_{fu}} \tag{32}$$

$$F_p = P_r.A_f.f_{fu} \tag{33}$$

The above mentioned upward deflection causes a tensile strain at the top fiber of the cross section. Therefore, after releasing the prestressing load, tensile stress at the concrete top fiber should not be larger than the concrete tensile strength (f_{ctm}), which can be ensured by accomplishing Eq. (34) where I is the moment of inertia of un-cracked section and $\varepsilon_{c0,vl}$ is the strain of the concrete top fiber due to the initial vertical loads.

$$f_{ctm} = \left[\frac{F_p . e . \frac{h}{2}}{I} - \frac{F_p}{b.h}\right] - E_c . \varepsilon_{c0,vl} \rightarrow P_r = \frac{f_{ctm} + E_c . \varepsilon_{c0,vl}}{A_f . f_{fu} . \left[\frac{e.h}{2.I} - \frac{1}{b.h}\right]} \rightarrow \frac{\varepsilon_p}{\varepsilon_{fu}} = \frac{f_{ctm} + E_c . \varepsilon_{c0,vl}}{A_f . f_{fu} . \left[\frac{e.h}{2.I} - \frac{1}{b.h}\right]} \rightarrow \tag{34}$$

$$\varepsilon_{p2} = \frac{(f_{ctm} + E_c . \varepsilon_{c0,vl}) . \varepsilon_{fu}}{A_f . f_{fu} . \left[\frac{e.h}{2.I} - \frac{1}{b.h}\right]}$$

4.2.2. Upper limit for the prestress level

The algorithm of the analytical approach described in previous section to determine the allowable prestress level is indicated in Fig. 16. The proposed analytical approach was applied to the prestressed RC slabs of the series A, B and C and an allowable prestress level (upper limit) applicable to the NSM CFRP laminates was obtained (Table 8).

It is verified that the concrete compressive strength has an important effect on limiting the maximum allowable prestress level in the NSM CFRP laminates in terms of $\varepsilon_{p2}/\varepsilon_{fu}$. In fact the parameter $\varepsilon_{p2}/\varepsilon_{fu}$ for the RC slabs with f_{cm} equal to 15 MPa and 39.5 MPa was, respectively, 60.6%, and 119.1%. The maximum allowable prestress level ($\varepsilon_p/\varepsilon_{fu}$) for the slabs of series A (f_{cm} = 39.5 MPa and ρ_{sl} = 0.39%), series B (f_{cm} = 15 MPa and ρ_{sl} = 0.39%) and series C (f_{cm} = 39.5 MPa and ρ_{sl} = 0.62%) was 56.2%, 52.5% and 55%, respectively, which indicates the tendency of the decrease of $\varepsilon_p/\varepsilon_{fu}$ either with the increase of the tensile steel reinforcement ratio or with the decrease of the concrete compressive strength.

4.3. Parametric study

In this section a parametric study is carried out in order to estimate the influence of the strength of the concrete (by using its average value of the compressive strength, f_{cm}) and the percentage of existing flexural reinforcement (ρ_{sl}) on the evaluation of the upper limit for the prestress level for ensuring a compromise of ductility and strengthening effectiveness of RC slabs flexurally strengthened with prestressed NSM CFRP laminates. It was tested five values for f_{cm} (20 MPa, 40 MPa, 60 MPa, 80 MPa and 100 MPa) and five values for ρ_{sl} (0.39%, 0.62%, 0.91%, 1.25% and 1.65%). The geometry of the RC slabs, the arrangement of the steel reinforcement, the material properties of the steel and CFRP, and the support and load conditions were the same ones of the specimens of the experimental program described in the section 2.

Table 9 displays, for each of the 25 RC slabs that were analyzed, the main results of the parametric study: the prestress level that assures a sufficient degree of the ductility for RC slabs flexurally strengthened with prestressed

NSM CFRP laminates ($\varepsilon_{p1}/\varepsilon_{fu}$); the prestress level that assures no cracks in the concrete ($\varepsilon_{p2}/\varepsilon_{fu}$). The adopted value for the upper limit for the prestress ($\varepsilon_{p}/\varepsilon_{fu}$) is the minimum of the values obtained for $\varepsilon_{p1}/\varepsilon_{fu}$ and $\varepsilon_{p2}/\varepsilon_{fu}$. Fig. 17 presents the influence of the f_{cm} (concrete strength) and the percentage of existing flexural reinforcement (ρ_{sl}) on the evaluation of the aforementioned upper limit for the prestress level ($\varepsilon_{p}/\varepsilon_{fu}$).

The values of Table 9 shows that $\varepsilon_{p2}/\varepsilon_{fu}$ is very sensitive to the concrete strength. In fact the values of $\varepsilon_{p2}/\varepsilon_{fu}$ for the RC slabs with f_{cm} equal to 20, 40, 60, 80 and 100 MPa were, respectively, 75.2%, 120.0%, 154.1%, 170.5% and 183.6%. Furthermore, according to the results of the Table 8, for the RC slabs of the series B (f_{cm} = 15 MPa) the obtained value of $\varepsilon_{p2}/\varepsilon_{fu}$ was 60.6%.

According to Fig. 17 and the values of Table 9 it is possible to conclude that regardless the strength of the concrete and the percentage of existing flexural reinforcement adopted, the maximum level of prestress is around 50% (ranged between 49.1% and 56.8%). The obtained results show that the upper limit for the prestress level ($\varepsilon_{p}/\varepsilon_{fu}$) decrease with the increase of ρ_{sl}, and, for each value of ρ_{sl} (until ρ_{sl} equal to 1.25%), $\varepsilon_{p}/\varepsilon_{fu}$ is almost insensitive to values of f_{cm} higher than 40 MPa.

5. CONCLUSIONS

To appraise the influence of the CFRP prestress level, concrete strength and percentage of existing flexural reinforcement on the performance of one-way RC slabs flexurally strengthened with prestressed NSM CFRP laminates, an extensive experimental program was carried out. An analytical formulation was developed for the prediction of the cracking, yielding and maximum loads of this type of structural elements. Additionally, a procedure was proposed to calculate an upper limit for the prestress level applicable to the CFRP laminates. From the obtained experimental results and the application of the analytical approach it is possible to extract the following conclusions:

- Regardless the CFRP prestress level, the strength of the concrete and the percentage of existing flexural reinforcement adopted in this experimental program, the NSM technique using CFRP laminates is highly effective for the flexural strengthening of RC slabs. In fact, the adopted CFRP strengthening configuration (ρ_f = 0.085%) has provided an increase of the maximum load ranged between 59% and 134%.
- A considerable increase of the load carrying capacity at service limit states (SLS) was observed in the strengthened RC slabs with the proposed technique. The adopted prestressed NSM CFRP configurations (ranged between 20%-50%) for the flexural strengthening of RC slabs with two concrete strength classes and two steel reinforcement ratios have increased the service load of the strengthened slabs from 42% to 190% of the service load of the reference slabs.

- In the strengthened RC slabs with prestressed CFRP laminates the deflection at maximum load (u_{Fmax}) was more than 1.6 times the deflection at yield initiation (u_{Fsy}), with substantial plastic incursion of the steel bars, which guarantees the required level of ductility for the RC slabs. However, it was verified a decrease of the ductility level of these slabs with the increase of the CFRP prestressed level.
- Regardless the CFRP prestress level, the strength of the concrete and the percentage of existing flexural reinforcement adopted in this experimental program, all strengthened slabs failed by the tensile rupture of the CFRP after yielding of the tensile steel reinforcements, indicating an excellent performance of the NSM CFRP technique for the flexural strengthening of RC slabs.
- When the same arrangements of NSM CFRP laminates were applied in slabs of concrete compressive strength (f_{cm}) equal to 15 MPa and in slabs of f_{cm} = 39.5 MPa, the obtained experimental results proved that the adopted strengthening technique is more effective in slabs with lower concrete strength class (f_{cm}=15 MPa), mainly at serviceability limit state (the average increase of the service load for the prestressed RC slabs with lower and higher compressive strength was, respectively, 157% and 99%).
- When the same arrangements of NSM CFRP laminates were applied in slabs with a percentage of the longitudinal tensile reinforcement (ρ_{sl}) equal to 0.39% (4ϕ8) and in slabs with ρ_{sl} equal to 0.62% (4ϕ10), the obtained experimental results showed that the adopted strengthening technique is more effective in the case of the slabs with lower percentage of the longitudinal bars, both for serviceability (the average increase of the service load for prestressed RC slabs with lower and higher ρ_{sl} was, respectively, 99% and 60%) and for ultimate limit states (the average increase of the maximum load for the prestressed RC slabs with lower and higher ρ_{sl} was, respectively, 129% and 61%).
- Taking into account the experimental results obtained in the tested slabs, the performance of a proposed analytical formulation for the prediction of the cracking, yielding and maximum loads of a RC slab flexurally strengthened using NSM technique with prestressed CFRP laminates was appraised. A very good predictive performance was obtained.
- A methodology to obtain an upper limit of the prestress level that can be applied to the CFRP laminates was proposed in order to ensure the aimed ductility performance of the prestressed RC slabs strengthened with NSM CFRP laminates. Furthermore, a parametric study was executed to highlight the influence of the percentage of existing tensile flexural reinforcement (ρ_{sl}) and the concrete strength (f_{cm}) on the evaluation of the upper limit for the prestress level for ensuring a compromise of ductility and strengthening effectiveness. Regardless the adopted values of ρ_{sl} and f_{cm}, the maximum level of prestress was around 50% (ranged between 49.1% and 56.8%). The

obtained results show that the upper limit for the prestress level ($\varepsilon_p/\varepsilon_{fu}$) decrease with the increase of ρ_{sl}, and, for each value of ρ_{sl} (until ρ_{sl} equal to 1.25%), $\varepsilon_p/\varepsilon_{fu}$ is almost insensitive to values of f_{cm} higher than 40 MPa.

ACKNOWLEDGEMENTS

The authors wish to acknowledge the support provided by the "Empreiteiros Casais" and S&P®. This work was supported by FEDER funds through the Operational Competitiveness and Internationalization Programme (POCI) and National Funds through FCT - Portuguese Foundation for Science and Technology under the project POCI-01-0145-FEDER-030956.

REFERENCES

[1] Bakis, C.E., Bank, L.C., Brown, V.L., Cosenza, E., Davalos, J.F., Lesko, J.J., Machida, A., Riskalla, S.H. and Triantafillou, T.C., *"Fiber-reinforced polymer composites for construction – state-of-the-art review"*, Journal of Composites for Construction, 6(2), pp. 73-87 (2002).

[2] Rahimi, H. and Hutchinson A., *"Concrete beams strengthened with externally bonded FRP plates"*, Journal of Composites for Construction, 5(1), pp. 44-56 (2001).

[3] M.R. Esfahani, M.R. Kianoush and A.R. Tajari, *"Flexural behaviour of reinforced concrete beams strengthened by CFRP sheets"*, Engineering Structures, 29(10), pp. 2428-2444 (2007).

[4] Barros, J.A.O., Dias, S.J.E. and Lima J.L.T., *"Efficacy of CFRP-based techniques for the flexural and shear strengthening of concrete beams"*, Journal Cement & Concrete Composites, 29(3), pp. 203-217 (2007).

[5] Bilotta, A., Ceroni, F., Nigro, E. and Pecce, M., *"Efficiency of CFRP NSM strips and EBR plates for flexural strengthening of RC beams and loading pattern influence"*, Composite Structures Journal, 124, pp. 163-175 (2015).

[6] Carolin, A., "*Carbon fibre reinforced polymers for strengthening of structural elements*", PhD Thesis, Division of Structural Engineering, Luleå University of Technology, Lulea, Sweden, 190 pp. (2003).

[7] El-Hacha, R. and Riskalla, S.H., "*Near-surface-mounted fiber-reinforced polymer reinforcements for flexural strengthening of concrete structures",* ACI Structural Journal, 101(5), pp. 717-726 (2004).

[8] Barros, J.A.O., Varma, R.K., Sena-Cruz, J.M. and Azevedo, A.F.M., "*Near surface mounted CFRP strips for the flexural strengthening of RC columns - experimental and numerical research*", Engineering Structures Journal, 30(12), pp. 3412-3425 (2008).

[9] Kotynia, R., *"Analysis of the flexural response of NSM FRP-strengthened concrete beams"*, 8th International

Symposium on Fiber Reinforced Polymer (FRP) Reinforcement for Concrete Structures (FRPRCS-8), Patras, Greece, July 16-18 (2007).

[10] Costa, I.G., Barros, J.A.O., "*Flexural and shear strengthening of RC beams with composites materials – the influence of cutting steel stirrups to install CFRP strips*", Cement and Concrete Composites Journal, 32, pp. 544-553 (2010).

[11] Sharaky, I.A., Torres, L. and Sallam, H.E.M., "*Experimental and analytical investigation into the flexural performance of RC beams with partially and fully bonded NSM FRP bars/strips*", Composites Structures Journal, 122, pp. 113-126 (2015).

[12] Bianco, V., Barros, J.A.O. and Monti, G., "*Three dimensional mechanical model for simulating the NSM FRP strips shear strength contribution to RC beams*", Engineering Structures Journal, 31(4), pp. 815-826 (2009).

[13] Bonaldo, E.; Barros, J.A.O. and Lourenço, P.J.B., *"Efficient strengthening technique to increase the flexural resistance of existing RC slabs"*, ASCE Composites for Construction Journal, 12(2), pp. 149-159 (2008).

[14] Dalfré, G.M. and Barros, J.A.O., *"NSM technique to increase the load carrying capacity of continuous RC slabs"*, Engineering Structures Journal, 56, pp. 137-153 (2013).

[15] Barros, J.A.O., "*Pre-stress technique for the flexural strengthening with NSM-CFRP strips*", 9th International Symposium on Fiber Reinforced Polymer Reinforcement for Concrete Structures, Sydney, Australia, paper 85, 13-15 July (2009).

[16] Badawi M. and Soudki K., "*Flexural strengthening of RC beams with prestressed NSM CFRP rods - Experimental and analytical investigation"*, Construction and Building Materials Journal, 23, pp. 3292-3300 (2009).

[17] El-Hacha, R. and Gaafar M., "*Flexural strengthening of reinforced concrete beams using prestressed, near-surface-mounted CFRP bars*", PCI Journal, Fall 2011.

[18] Hajihashemi, A., Mostofinejad, D. and Azhari, M., *"Investigation of RC Beams Strengthened with Prestressed NSM CFRP Laminates"*, ASCE Composites for Construction Journal, 15(6), pp. 887-895 (2011).

[19] Rezazadeh, M. A.; Costa, I.G.; Barros, J.A.O., "*Influence of prestress level on NSM CFRP laminates for the flexural strengthening of RC beams*", Composite Structures Journal, 116(1), pp. 489-500 (2014).

[20] Hosseini M.R.M., Dias, S.J.E. and Barros, J.A.O., *"Effectiveness of prestressed NSM CFRP laminates for the flexural strengthening of RC slabs"*, Composite Structures Journal, 111, pp. 249-258 (2014).

[21] ACI (American Concrete Institute), 2011, "*Building code requirements for structural concrete*", ACI-318, Farmington Hills, MI.

[22] EN 206-1, *"Concrete - Part 1: Specification, performance, production and conformity",* European standard, CEN, 69 pp. (2000).

[23] LNEC E397-1993, *"Concrete - Determination of the elasticity modulus under compression",* Portuguese specification from LNEC (1993).

[24] EN 10002-1, *"Metallic materials - Tensile testing. Part 1: Method of test (at ambient temperature)"*, European Standard, CEN, Brussels, Belgium, 35 pp. (1990).

[25] ISO 527-5, *"Plastics - Determination of tensile properties - Part 5: Test conditions for unidirectional fibre-reinforced plastic composites"*, International Organization for Standardization (ISO), Geneva, Switzerland, 9 pp. (1997).

[26] Costa, I.G. and Barros, J.A.O., *"Tensile creep of a structural epoxy adhesive: experimental and analytical characterization"*, International Journal of Adhesion & Adhesives, 59, pp. 115-124 (2015).

[27] ISO 527-2, "*Plastics - Determination of tensile properties - Part 2: Test conditions for moulding and extrusion plastics*", International Organization for Standardization (1993).

[28] EN 1992-1-1, "*Eurocode2: Design of Concrete Structures Parte 1-1: General Rules for Buildings*", CEN, Brussels, Belgium (2004).

[29] ACI 440.2R-08, 2008, *"Guide for the Design and Construction of Externally Bonded FRP Systems for Strengthening Concrete Structures"*, Reported by ACI (American Concrete Institute) Committee 440, Farmington Hills, MI.

FIGURES AND TABLES

List of Figures:

Fig. 1 - Geometry of the slabs, steel reinforcements common to all of the tested slabs, support and load conditions (dimensions in mm).

Fig. 2 - a) NSM CFRP flexural strengthening configuration (dimensions in mm), b) application of passive NSM CFRP laminates, c) application of the prestress in the NSM CFRP laminates, d) and e) test-setup.

Fig. 3 - Positions of the: a) displacement transducers (LVDTs); b) strain gauges in the monitored longitudinal tensile steel bars; c) strain gauges in the NSM CFRP laminates of non-prestressed slab; d) strain gauges in the NSM CFRP laminates of prestressed slabs (dimensions in mm).

Fig. 4 - Load *vs.* deflection at mid-span of the tested RC slabs of series: a) A, b) B, c) C.

Fig. 5 - Crack patterns of the tested RC slabs (series A).

Fig. 6 - Failure modes of the tested RC slabs.

Fig. 7 - Effect of the prestress level on: a) cracking, service, yielding and ultimate loads; and b) yielding and ultimate deflection (Series A).

Fig. 8 - Influence of the prestress level on the (series A): a) normalized absorption energy; b) ductility index of prestressed versus non-prestressed slabs.

Fig. 9 - Influence of the concrete strength in the effectiveness of the prestressed NSM CFRP laminates in terms of: a) cracking load; b) service load; c) yielding load; d) maximum load; and e) maximum deflection.

Fig. 10 - Influence of the percentage of flexural reinforcement in the effectiveness of the prestressed NSM CFRP laminates in terms of: a) cracking load; b) service load; c) yielding load; d) maximum load; and e) maximum deflection.

Fig. 11 - Strain and stress diagram of the cross section and force components at crack initiation state.

Fig. 12 - Strain and stress diagram of the cross section and force components at yield initiation state.

Fig. 13 - Strain and stress diagram of the cross section and force components at failure state, based on ACI 440.2R-08 [29] (FRP rupture as a failure mode).

Fig. 14 - Experimental *vs.* analytical results of: a) cracking load in series of slabs; b) cracking load for the prestress levels; c) yielding load in series of slabs; d) yielding load for the prestress levels; e) maximum load in series of slabs; f) maximum load for the prestress levels.

Fig. 15 - Strain profile of the cross section and force components at ultimate stage adopting rupture of the CFRP reinforcement based on ACI 440.2R-08 [29].

Fig. 16 - Algorithm of the analytical model to determine the allowable prestress level.

Fig. 17 - Influence of the ρ_{sl} and f_{cm} on the evaluation of the upper limit for the prestress level for ensuring a compromise of ductility and strengthening effectiveness.

List of Tables:

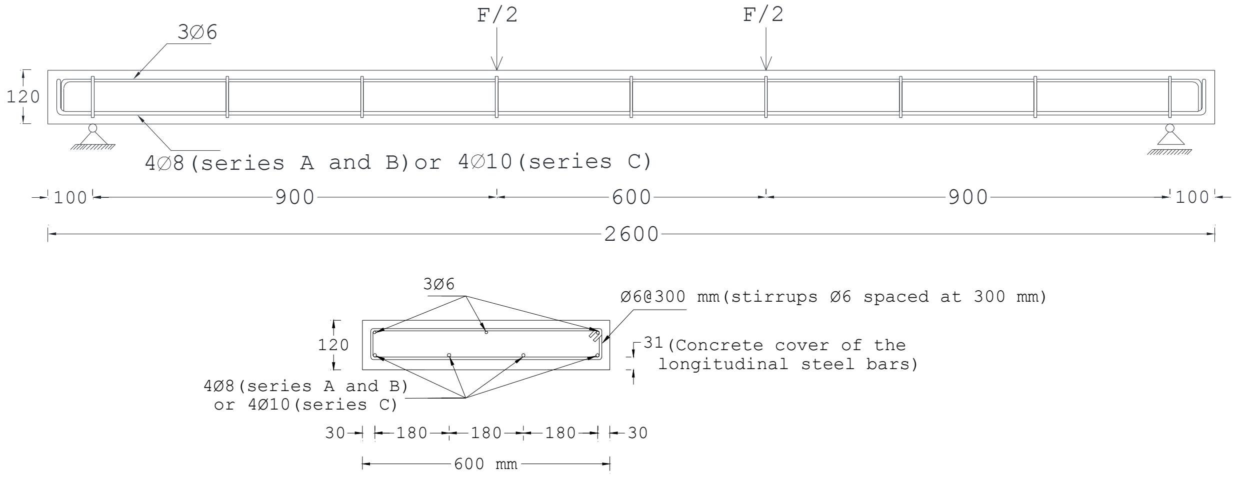

Fig. 1 - Geometry of the slabs, steel reinforcements common to all of the tested slabs, support and load conditions (dimensions in mm).

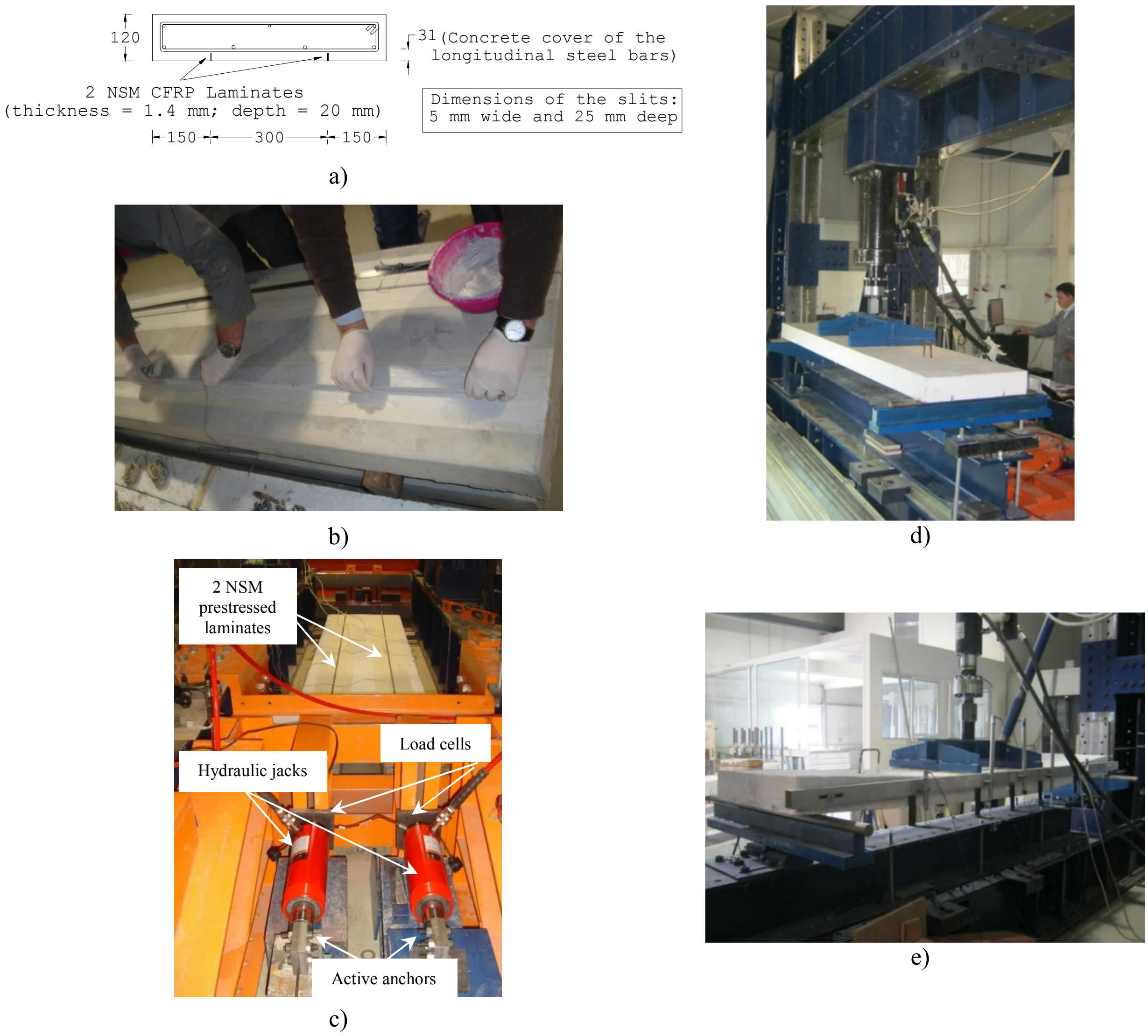

Fig. 2 - a) NSM CFRP flexural strengthening configuration (dimensions in mm), b) application of passive NSM CFRP laminates, c) application of the prestress in the NSM CFRP laminates, d) and e) test-setup.

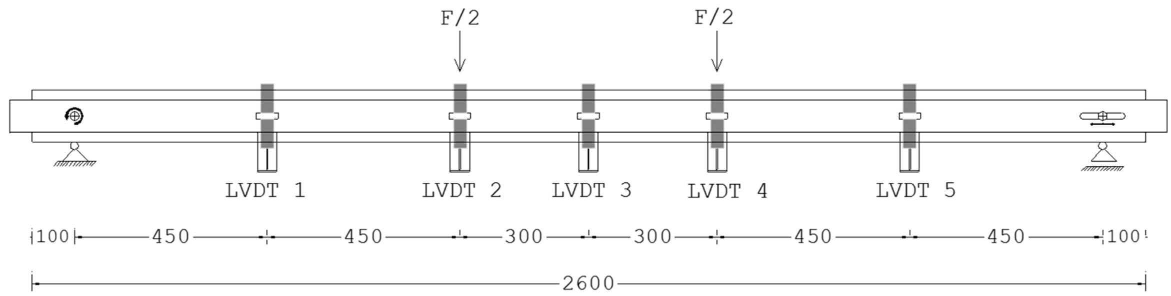

a)

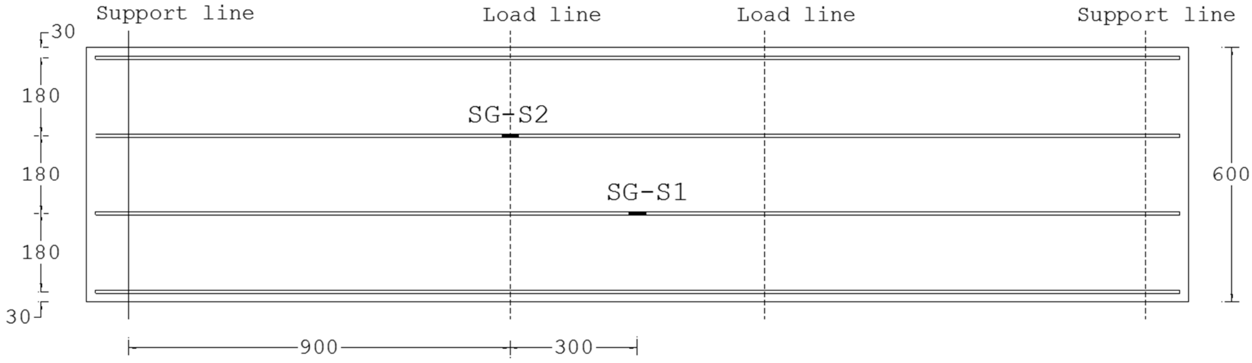

b) Bottom view: showing only the longitudinal tensile bars

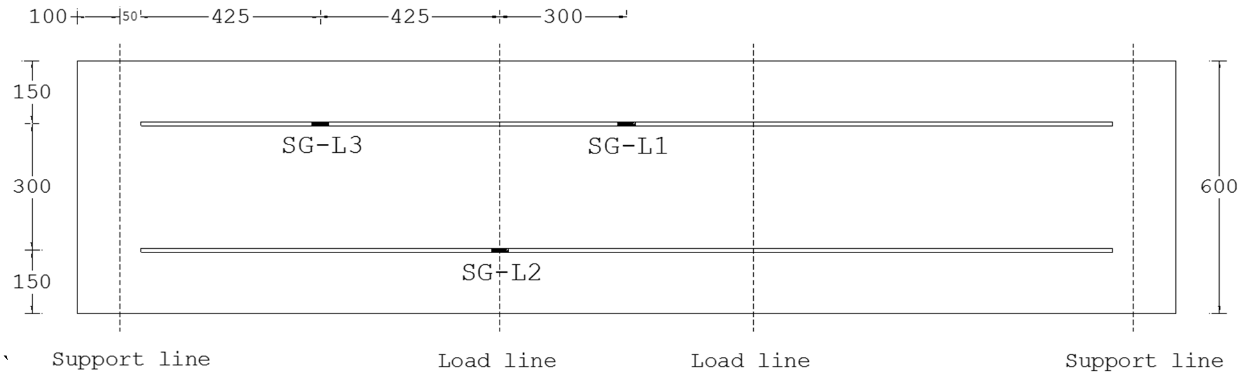

c) Bottom view: showing only two CFRP laminates in non-prestressed slab

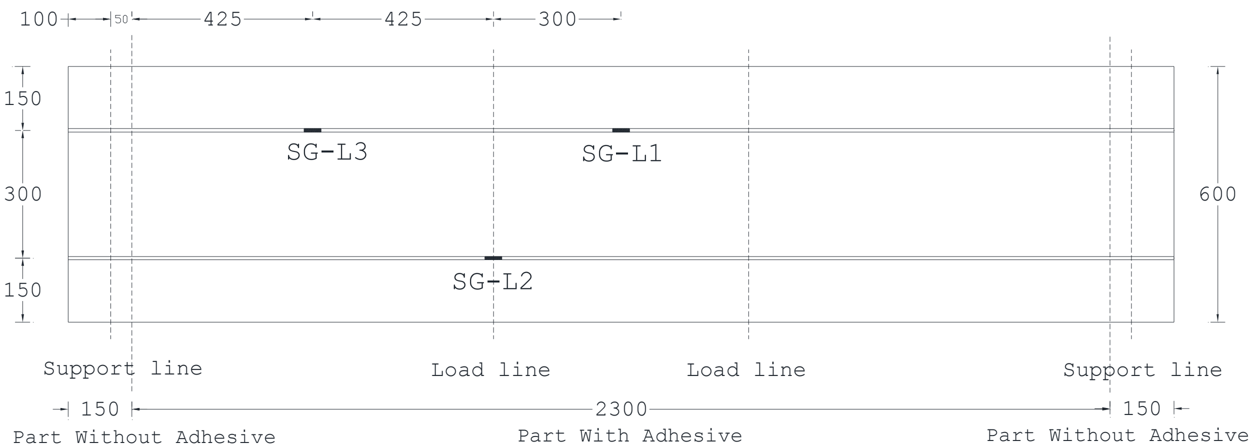

d) Bottom view: showing only two CFRP laminates in prestressed slabs

Fig. 3 - Positions of the: a) displacement transducers (LVDTs); b) strain gauges in the monitored longitudinal tensile steel bars; c) strain gauges in the NSM CFRP laminates of non-prestressed slab; d) strain gauges in the NSM CFRP laminates of prestressed slabs (dimensions in mm).

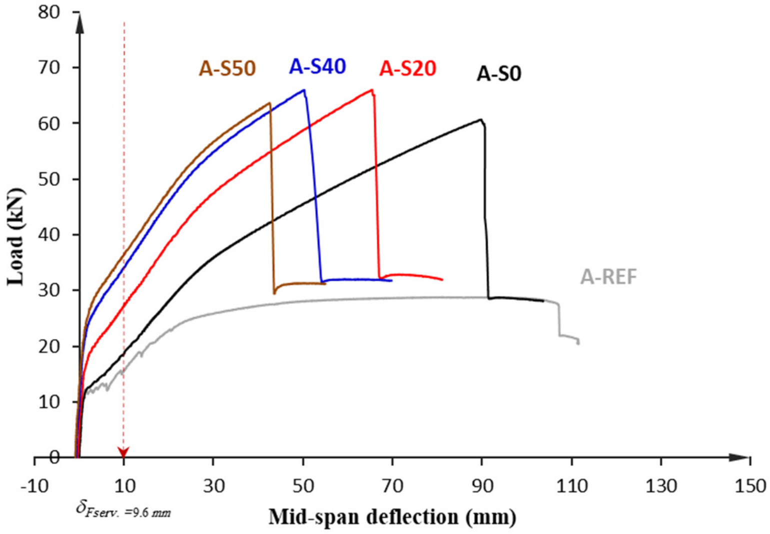

a)

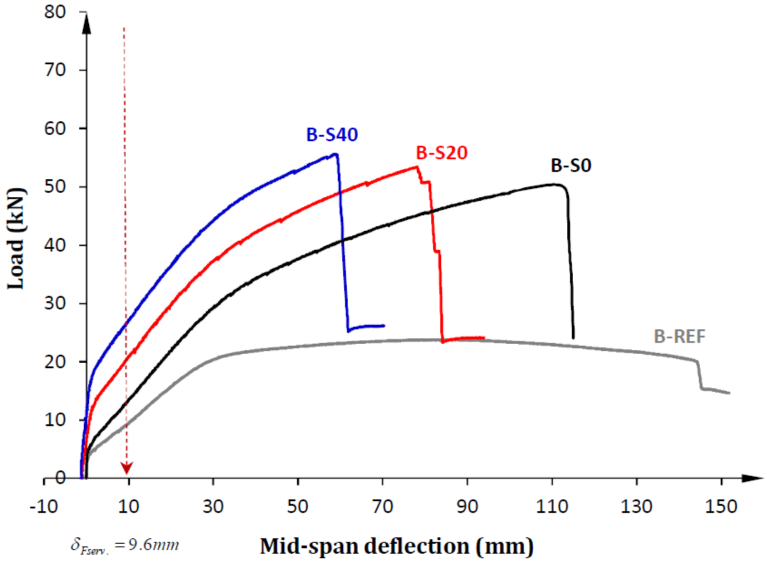

b)

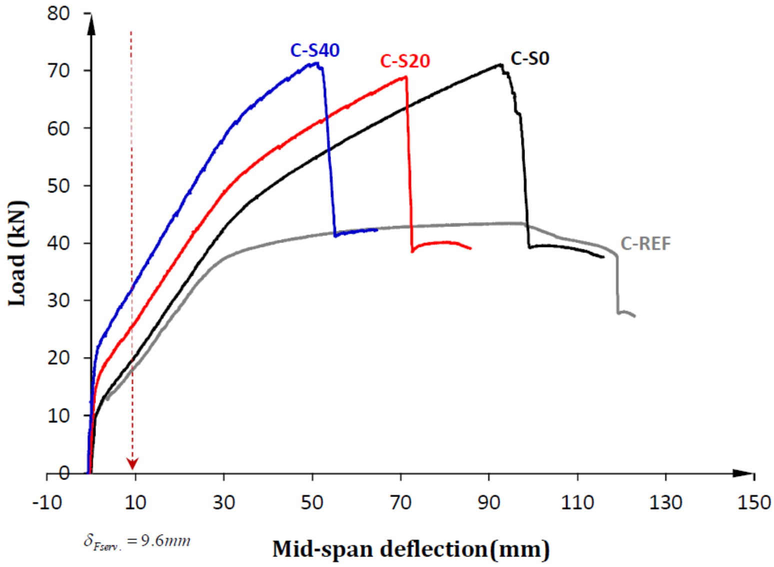

c)

Fig. 4 - Load *vs.* deflection at mid-span of the tested RC slabs of series: a) A, b) B, c) C.

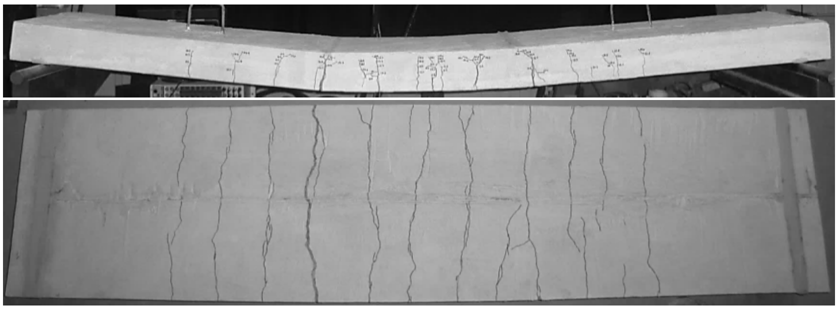

Non-strengthened RC slab (A-REF)

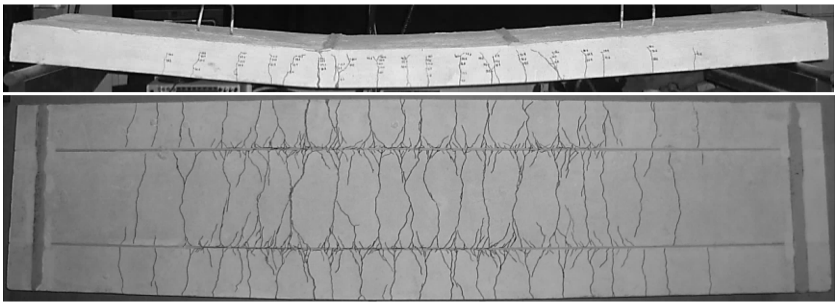

RC slab strengthened with non-prestressed CFRP laminates (A-S0)

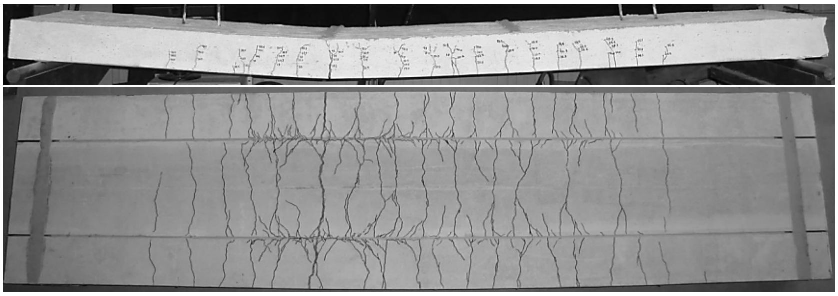

RC slab strengthened with prestressed CFRP laminates - 20% (A-S20)

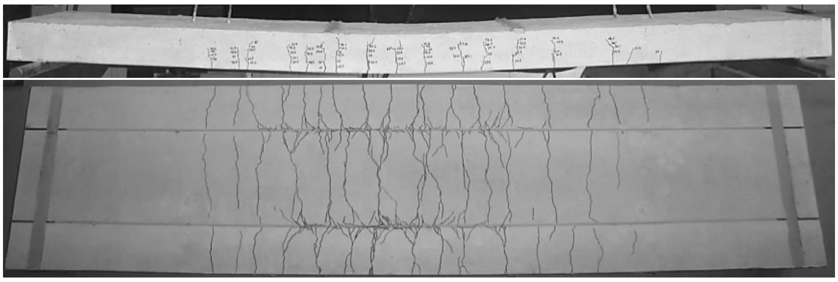

RC slab strengthened with prestressed CFRP laminates - 40% (A-S40)

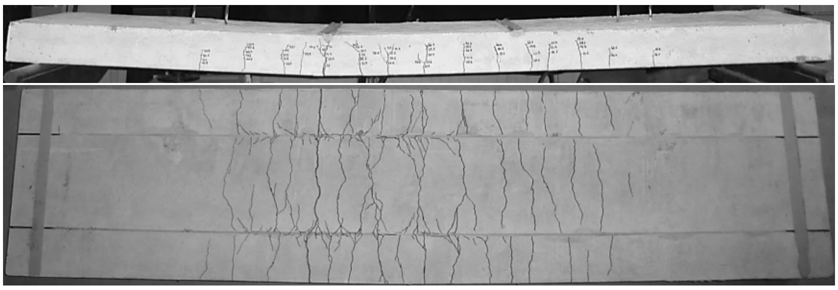

RC slab strengthened with prestressed CFRP laminates - 50% (A-S50)

Fig. 5 - Crack patterns of the tested RC slabs (series A).

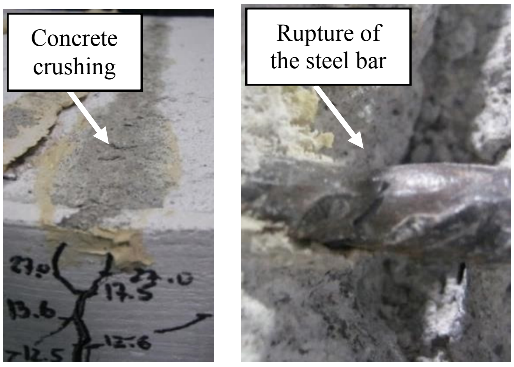

a) Concrete crushing and tensile rupture of a steel bar in the reference RC slab

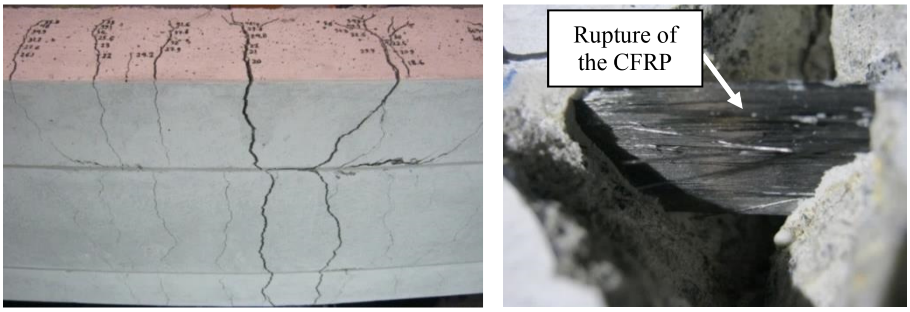

b) Rupture of the CFRP in the slabs strengthened with NSM CFRP laminates

Fig. 6 - Failure modes of the tested RC slabs.

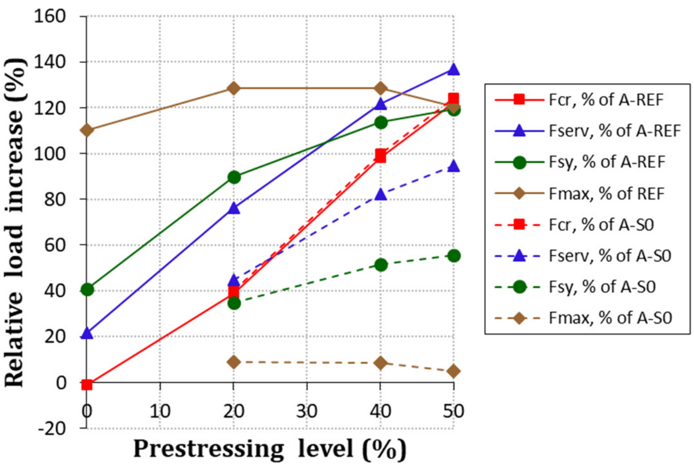

a)

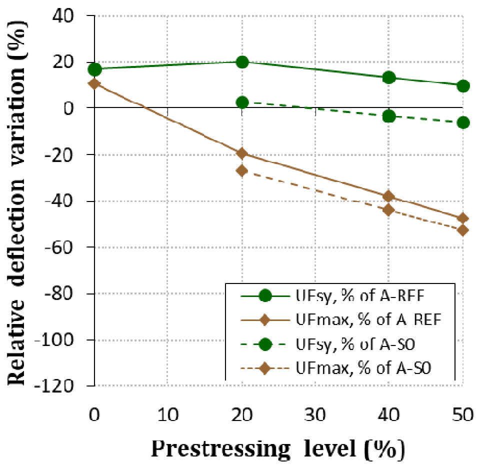

b)

Fig. 7 - Effect of the prestress level on: a) cracking, service, yielding and ultimate loads; and b) yielding and ultimate deflection (Series A).

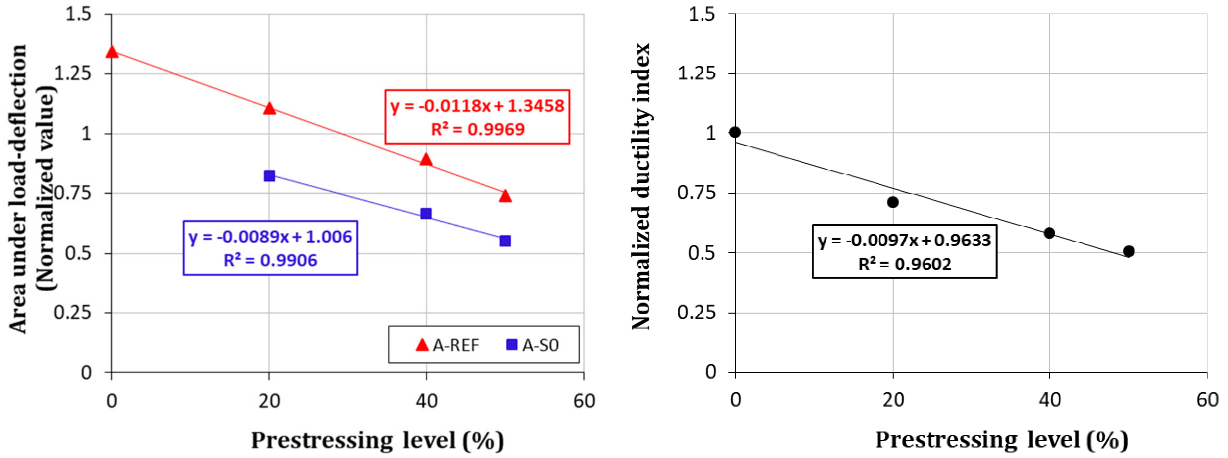

a) b)

Fig. 8 - Influence of the prestress level on the (series A): a) normalized absorption energy; b) ductility index of prestressed versus non-prestressed slabs.

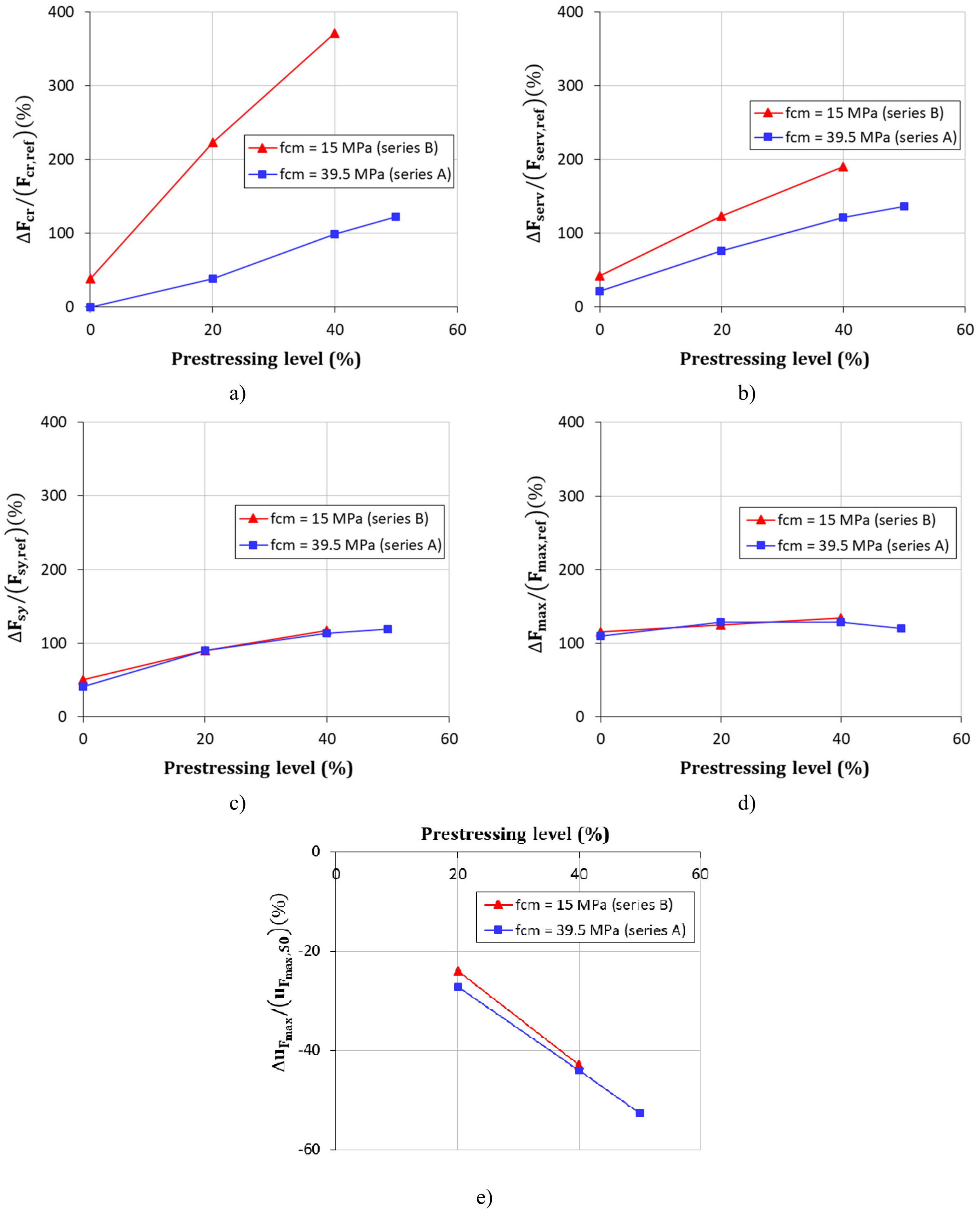

Fig. 9 - Influence of the concrete strength in the effectiveness of the prestressed NSM CFRP laminates in terms of: a) cracking load; b) service load; c) yielding load; d) maximum load; and e) maximum deflection.

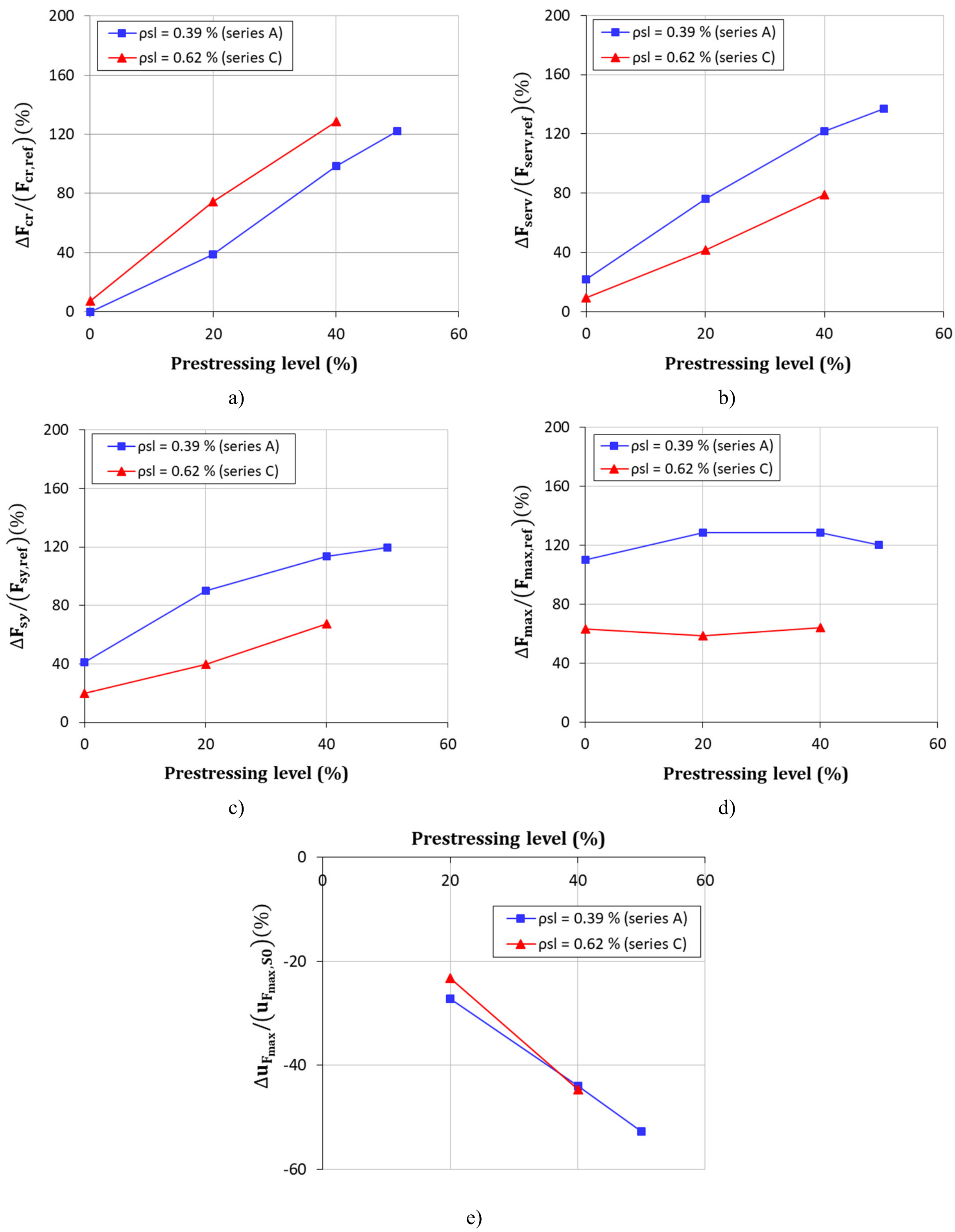

Fig. 10 - Influence of the percentage of flexural reinforcement in the effectiveness of the prestressed NSM CFRP laminates in terms of: a) cracking load; b) service load; c) yielding load; d) maximum load; and e) maximum deflection.

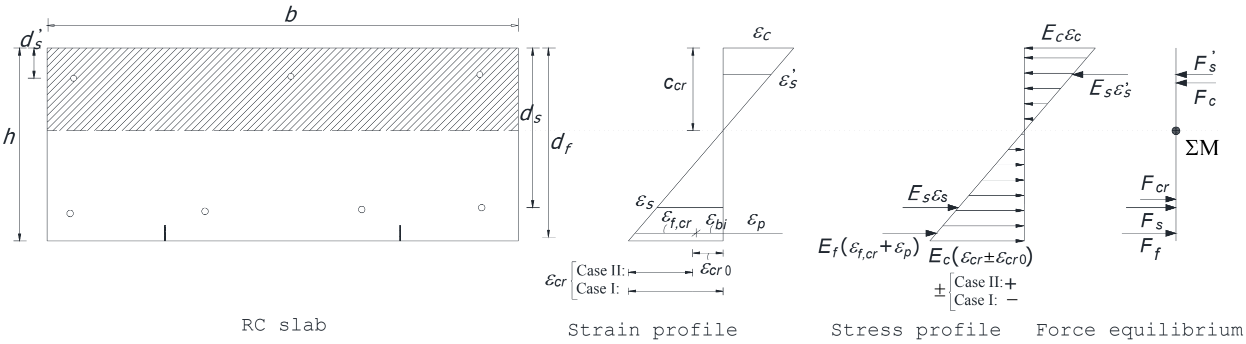

Fig. 11 - Strain and stress diagram of the cross section and force components at crack initiation state.

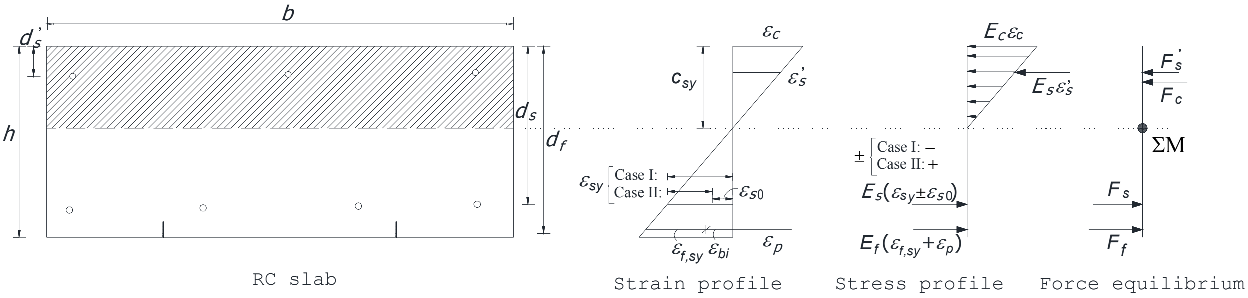

Fig. 12 - Strain and stress diagram of the cross section and force components at yield initiation state.

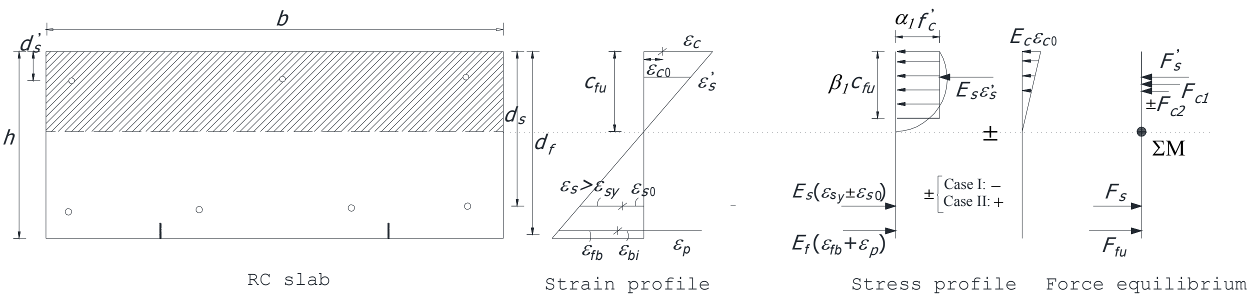

Fig. 13 - Strain and stress diagram of the cross section and force components at failure state, based on ACI 440.2R-08 [29] (FRP rupture as a failure mode).

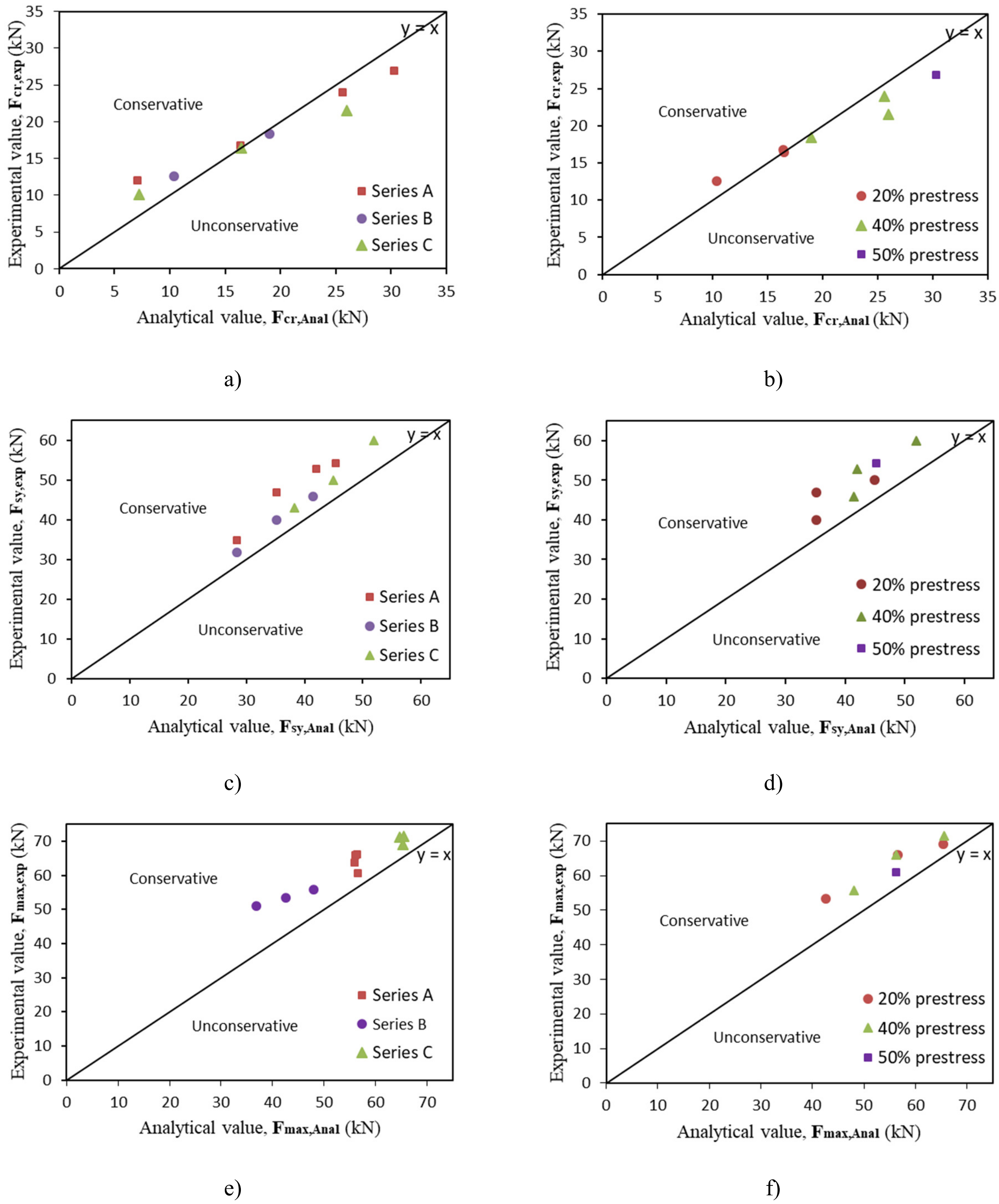

Fig. 14 - Experimental *vs.* analytical results of: a) cracking load in series of slabs; b) cracking load for the prestress levels; c) yielding load in series of slabs; d) yielding load for the prestress levels; e) maximum load in series of slabs; f) maximum load for the prestress levels.

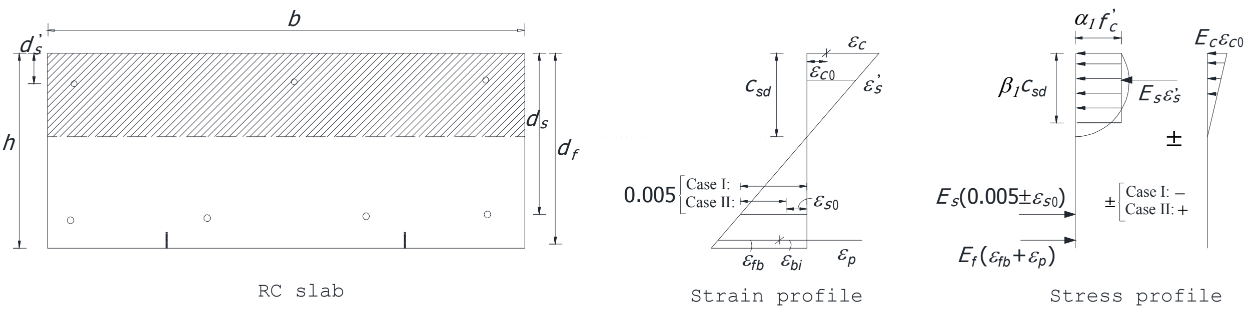

Fig. 15 - Strain profile of the cross section and force components at ultimate stage adopting rupture of the CFRP reinforcement based on ACI 440.2R-08 [29].

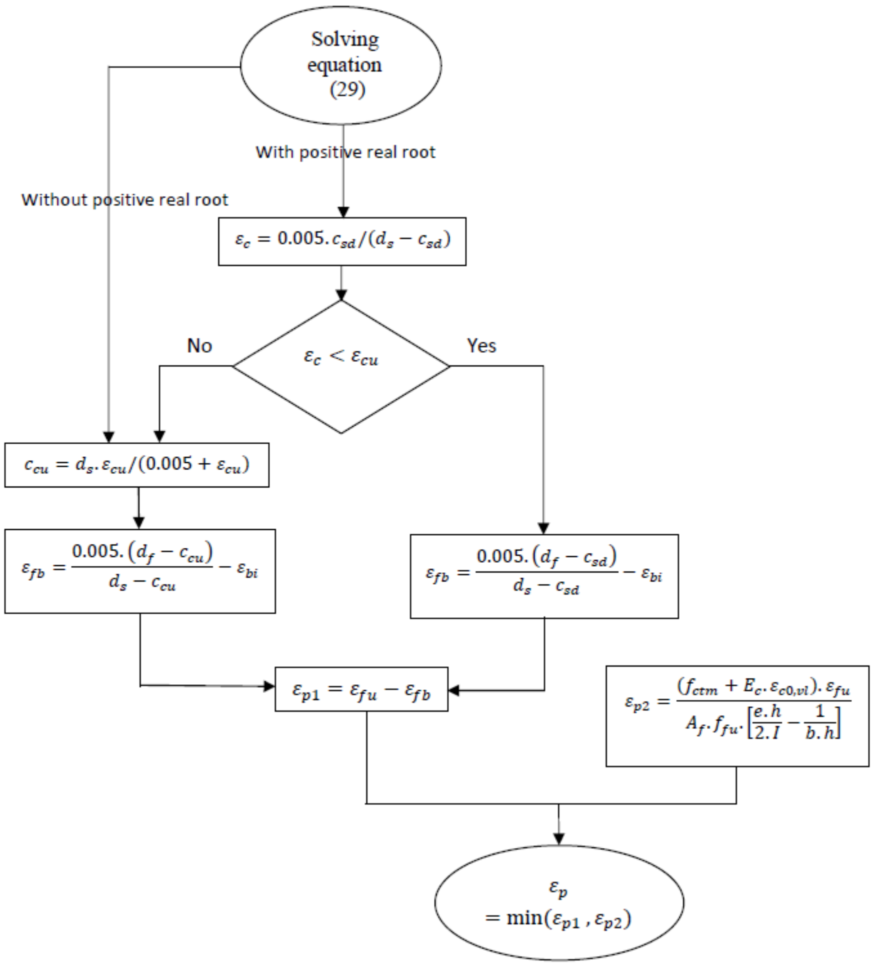

Fig. 16 - Algorithm of the analytical model to determine the allowable prestress level.

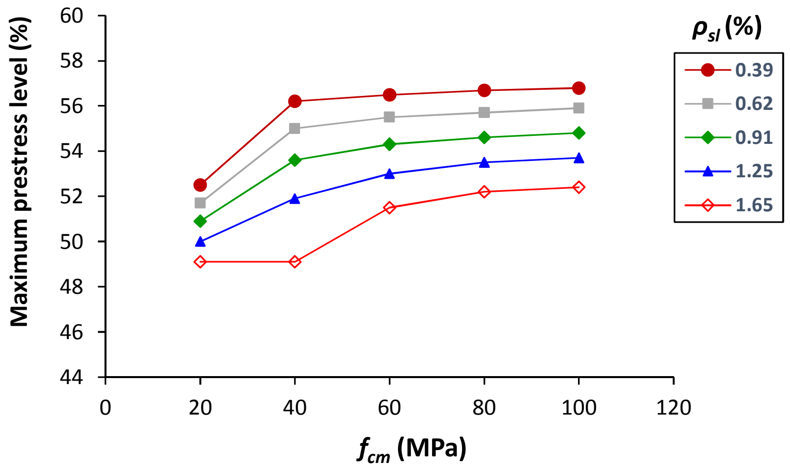

Fig. 17 - Influence of the ρ_{sl} and f_{cm} on the evaluation of the upper limit for the prestress level for ensuring a compromise of ductility and strengthening effectiveness.

Table 1 - General information of the RC slabs of series A, B and C.

Series	Slab	f_{cm} (MPa)	ρ_{sl} (%) (1)	NSM CFRP flexural strengthening		Level of prestress (%)
				Quantity	ρ_f (%) (2)	
Series A	A-REF	39.5	0.394	-	-	-
	A-S0			2 CFRP laminates of 1.4×20 mm^2 cross section (A_f = 2×1.4×20 = 56 mm^2)	0.085	0
	A-S20					20
	A-S40					40
	A-S50					50
Series B	B-REF	15.0	0.394	-	-	-
	B-S0			2 CFRP laminates of 1.4×20 mm^2 cross section (A_f = 2×1.4×20 = 56 mm^2)	0.085	0
	B-S20					20
	B-S40					40
Series C	C-REF	39.5	0.623	-	-	-
	C-S0			2 CFRP laminates of 1.4×20 mm^2 cross section (A_f = 2×1.4×20 = 56 mm^2)	0.085	0
	C-S20					20
	C-S40					40

(1) The percentage of the existing flexural reinforcement was obtained from $\rho_{sl} = \left(A_{sl}/\left(b_w \times d_s\right)\right)\times 100$, where A_{sl} is the cross sectional area of the longitudinal tensile steel reinforcement (see Fig. 1), b_w = 600 mm is the width of the slab's cross section, and d_s is the distance from extreme compression fibre to the centroid of tensile reinforcement.

(2) The CFRP percentage was obtained from $\rho_f = \left(A_f/\left(b_w \times d_f\right)\right)\times 100$, where A_f is the cross sectional area of the NSM CFRP laminates and d_f is the distance from extreme compression fibre to the centroid of the NSM CFRP laminates.

Table 2 - Summary of the results in terms of load carrying capacity and deflection performance.

Series	Slab	Cracking	Service	Yielding		Maximum	
		F_{cr} (kN) (1)	F_{serv} (kN) (1)	F_{sy} (kN) (1)	u_{Fsy} (mm)	F_{max} (kN)	u_{Fmax} (mm)
A	A-REF	12.1 (0.42)	15.2 (0.53)	24.7 (0.85)	24.2	28.9	81.1
	A-S0	12.1 (0.20)	18.5 (0.30)	34.8 (0.57)	28.3	60.7	89. 8
	A-S20	16.8 (0.25)	26.8 (0.41)	46.9 (0.71)	29.1	66.1	65.4
	A-S40	24.0 (0.36)	33.7 (0.51)	52.8 (0.80)	27.4	66.0	50.3
	A-S50	26.9 (0.42)	36.0 (0.57)	54.2 (0.85)	26.6	63.7	42.5
B	B-REF	3.9 (0.16)	9.2 (0.39)	21.1 (0.89)	29.8	23.8	85.5
	B-S0	5.4 (0.11)	13.1 (0.26)	31.8 (0.62)	32.0	51.1	102.9
	B-S20	12.6 (0.24)	20.5 (0.38)	40.0 (0.75)	31.5	53.4	78.2
	B-S40	18.4 (0.33)	26.7 (0.48)	45.9 (0.82)	31.5	55.7	58.8
C	C-REF	9.4 (0.22)	18.2 (0.42)	35.8 (0.82)	27.5	43.5	97.0
	C-S0	10.1 (0.14)	19.9 (0.28)	42.9 (0.60)	30.5	71.1	92.8
	C-S20	16.4 (0.24)	25.8 (0.37)	50.0 (0.72)	31.5	69.0	71.2
	C-S40	21.5 (0.30)	32.6 (0.46)	60.0 (0.84)	31.4	71.4	51.3

(1) The values in parenthesis are percentage of related F_{max}.

Table 3 - Maximum strain values recorded in CFRP laminates's strain gauges up to the maximum load of the slabs.

Series	Slab	SG-L1 (‰)			SG-L2 (‰)			SG-L3 (‰)		
		Prestressing	Test	Total	Prestressing	Test	Total	Prestressing	Test	Total
A	A-S0	0.0	15.1	15.1	0.0	14.9	14.9	0.0	5.7	5.7
	A-S20	3.0	11.1	14.1	3.0	12.2	15.2	3.0	4.8	7.8
	A-S40	6.0	9. 6	15.5	5.9	9.0	14.9	6.1	2.1	8.2
	A-S50	7.5	8.0	15.5	7.5	8.4	15.9	7.4	2.0	9.4
B	B-S0	0.0	14.6	14.6	0.0	14.6	14.6	0.0	4.7	4.7
	B-S20	3.1	11.9	14.9	3.2	11.8	15.0	3.1	4.0	7.1
	B-S40	5.9	9.1	14.9	5.9	9.9	15.8	6.0	2.9	8.9
C	C-S0	0.0	15.0	15.0	0.0	14.5	14.5	0.0	5.0	5.0
	C-S20	3.0	11.7	14.7	3.1	11.9	15.0	3.0	3.6	6.6
	C-S40	6.1	10.3	16.4	6.0	8.5	14.5	5.6	2.5	8.1

Table 4 - Influence of the prestress level in the effectiveness of prestressed NSM CFRP laminates technique.

Slab	Level of prestress	$\Delta F_{cr}/F_{cr}^{Ref}$ (%)	$\Delta F_{serv}/F_{serv}^{Ref}$ (%)	$\Delta F_{sy}/F_{sy}^{Ref}$ (%)	$\Delta F_{max}/F_{max}^{Ref}$ (%)	$\Delta u_{F_{max}}/u_{F_{max}}^{Ref}$ (%)
A-S0	0%	0	21.7	40.9	110.0	10.8
A-S20	20%	38.8	76.3	89.9	128.7	-19.3
A-S40	40%	98.3	121.7	113.8	128.4	-37.9
A-S50	50%	122.3	136.8	119.4	120.4	-47.5

Table 5 - Influence of the concrete strength (f_{cm}) in the effectiveness of the prestressed NSM CFRP laminates.

Level of prestress	$\Delta F_{cr}/F_{cr}^{Ref}$ (%) (1)		$\Delta F_{serv}/F_{serv}^{Ref}$ (%) (2)		$\Delta F_{sy}/F_{sy}^{Ref}$ (%) (3)		$\Delta F_{max}/F_{max}^{Ref}$ (%) (4)		$\Delta u_{F_{max}}/u_{F_{max}}^{S0}$ (%) (5)	
	f_{cm} = 15 MPa	f_{cm} =39.5 MPa	f_{cm} = 15 MPa	f_{cm} =39.5 MPa	f_{cm} = 15 MPa	f_{cm} = 39.5 MPa	f_{cm} = 15 MPa	f_{cm} = 39.5 MPa	f_{cm} = 15 MPa	f_{cm} = 39.5 MPa
0%	38.5	0	42.4	21.7	50.7	40.9	114.7	110.0	-	-
20%	223.1	38.8	122.8	76.3	89.6	89.9	124.4	128.7	-24.0	-27.1
40%	371.8	98.3	190.2	121.7	117.5	113.8	134.0	128.4	-42.9	-44.0

(1) $\Delta F_{cr} = F_{cr}^{Str} - F_{cr}^{Ref}$; (2) $\Delta F_{serv} = F_{serv}^{Str} - F_{serv}^{Ref}$; (3) $\Delta F_{sy} = F_{sy}^{Str} - F_{sy}^{Ref}$; (4) $\Delta F_{max} = F_{max}^{Str} - F_{max}^{Ref}$; (5) $\Delta u_{F_{max}} = u_{F_{max}}^{Str} - u_{F_{max}}^{S0}$, where $u_{F_{max}}^{S0}$ is the deflection corresponding to F_{max}^{Str} of the strengthened slab without prestressed (A-S0 in series A and B-S0 in series B). The meaning of the others parameters was described in previous section.

Table 6 - Influence of the percentage of flexural reinforcement (ρ_{sl}) in the effectiveness of the prestressed NSM CFRP laminates.

Level of prestress	$\Delta F_{cr}/F_{cr}^{Ref}$ (%) (1)		$\Delta F_{serv}/F_{serv}^{Ref}$ (%) (2)		$\Delta F_{sy}/F_{sy}^{Ref}$ (%) (3)		$\Delta F_{max}/F_{max}^{Ref}$ (%) (4)		$\Delta u_{F_{max}}/u_{F_{max}}^{S0}$ (%) (5)	
	ρ_{sl} =0.39% (4ϕ8)	ρ_{sl} =0.62% (4ϕ10)	ρ_{sl} =0.39% (4ϕ8)	ρ_{sl} =0.62% (4ϕ10)	ρ_{sl} =0.39% (4ϕ8)	ρ_{sl} =0.62% (4ϕ10)	ρ_{sl} =0.39% (4ϕ8)	ρ_{sl} =0.62% (4ϕ10)	ρ_{sl} =0.39% (4ϕ8)	ρ_{sl} =0.62% (4ϕ10)
0%	0	7.4	21.7	9.3	40.9	19.8	110.0	63.4	-	-
20%	38.8	74.5	76.3	41.8	89.9	39.7	128.7	58.6	-27.1	-23.3
40%	98.3	128.7	121.7	79.1	113.8	67.6	128.4	64.1	-44.0	-44.7

(1) $\Delta F_{cr} = F_{cr}^{Str} - F_{cr}^{Ref}$; (2) $\Delta F_{serv} = F_{serv}^{Str} - F_{serv}^{Ref}$; (3) $\Delta F_{sy} = F_{sy}^{Str} - F_{sy}^{Ref}$; (4) $\Delta F_{max} = F_{max}^{Str} - F_{max}^{Ref}$; (5) $\Delta u_{F_{max}} = u_{F_{max}}^{Str} - u_{F_{max}}^{S0}$, where $u_{F_{max}}^{S0}$ is the deflection corresponding to F_{max}^{Str} of the strengthened slab without prestressed (A-S0 in series A and C-S0 in series C). The meaning of the others parameters was described in previous section.

Table 7 - Experimental *vs.* analytical results in terms of cracking, yielding and maximum loads.

Series	Slab	Cracking load			Yielding load			Maximum load		
		$F_{cr,exp}$ (kN)	$F_{cr,Anal}$ (kN)	$F_{cr,exp}/F_{cr,Anal}$	$F_{sy,exp}$ (kN)	$F_{sy,Anal}$ (kN)	$F_{sy,exp}/F_{sy,Anal}$	$F_{max,exp}$ (kN)	$F_{max,Anal}$ (kN)	$F_{max,exp}/F_{max,Anal}$
Series A	A-S0	12.1	7.1	1.70	34.8	28.4	1.23	60.7	56.6	1.07
	A-S20	16.8	16.4	1.02	46.9	35.2	1.33	66.1	56.5	1.17
	A-S40	24.0	25.6	0.94	52.8	42.0	1.26	66.0	56.2	1.17
	A-S50	26.9	30.3	0.89	54.2	45.3	1.20	63.7	56.0	1.14
Series B	B-S0	5.4	0.8	6.75	31.8	28.3	1.12	51.1	36.9	1.38
	B-S20	12.6	10.4	1.21	40.0	35.2	1.14	53.4	42.6	1.25
	B-S40	18.4	19.0	0.97	45.9	41.5	1.11	55.7	48.0	1.16
Series C	C-S0	10.1	7.2	1.40	42.9	38.2	1.12	71.1	64.7	1.10
	C-S20	16.4	16.5	0.99	50.0	44.9	1.11	69.0	65.4	1.06
	C-S40	21.5	26.0	0.83	60.0	51.9	1.16	71.4	65.5	1.09
Bias		λ_p		1.11	λ_p		1.18	λ_p		1.16
Coefficient variation		V_P		0.26	V_P		0.06	V_P		0.08

Table 8 - Allowable prestress level for the series of the tests (A, B and C).

Series	Series A	Series B	Series C
$\varepsilon_{p1}/\varepsilon_{fu}$ (%)	56.1	52.5	55.0
$\varepsilon_{p2}/\varepsilon_{fu}$ (%)	119.1	60.6	119.1
Max. prestress level (%)	56.1	52.5	55.0

Table 9 - Results of the parametric study about the maximum level of prestress.

f_{cm} (MPa)	Tensile steel reinforcement (Ratio of tensile steel reinforcement -ρ_{sl})														
	4ϕ8 (ρ_{sl} = 0.39%)			4ϕ10 (ρ_{sl} = 0.62%)			4ϕ12 (ρ_{sl} = 0.91%)			4ϕ14 (ρ_{sl} = 1.25%)			4ϕ16 (ρ_{sl} = 1.65%)		
	$\varepsilon_{p1}/\varepsilon_{fu}$ (%)	$\varepsilon_{p2}/\varepsilon_{fu}$ (%)	$\varepsilon_{p}/\varepsilon_{fu}$ (%) (1)	$\varepsilon_{p1}/\varepsilon_{fu}$ (%)	$\varepsilon_{p2}/\varepsilon_{fu}$ (%)	$\varepsilon_{p}/\varepsilon_{fu}$ (%) (1)	$\varepsilon_{p1}/\varepsilon_{fu}$ (%)	$\varepsilon_{p2}/\varepsilon_{fu}$ (%)	$\varepsilon_{p}/\varepsilon_{fu}$ (%) (1)	$\varepsilon_{p1}/\varepsilon_{fu}$ (%)	$\varepsilon_{p2}/\varepsilon_{fu}$ (%)	$\varepsilon_{p}/\varepsilon_{fu}$ (%) (1)	$\varepsilon_{p1}/\varepsilon_{fu}$ (%)	$\varepsilon_{p2}/\varepsilon_{fu}$ (%)	$\varepsilon_{p}/\varepsilon_{fu}$ (%) (1)
20	52.5	75.2	52.5	51.7	75.2	51.7	50.9	75.2	50.9	50.0	75.2	50.0	49.1	75.2	49.1
40	56.2	120.0	56.2	55.0	120.0	55.0	53.6	120.0	53.6	51.9	120.0	51.9	49.1	120.0	49.1
60	56.5	154.1	56.5	55.5	154.1	55.5	54.3	154.1	54.3	53.0	154.1	53.0	51.5	154.1	51.5
80	56.7	170.5	56.7	55.7	170.5	55.7	54.6	170.5	54.6	53.5	170.5	53.5	52.2	170.5	52.2
100	56.8	183.6	56.8	55.9	183.6	55.9	54.8	183.6	54.8	53.7	183.6	53.7	52.4	183.6	52.4

(1) Max. prestress level.